



Contents lists available at ScienceDirect

## CIRP Annals - Manufacturing Technology

journal homepage: <http://ees.elsevier.com/cirp/default.asp>



# Multiscale analyses and characterizations of surface topographies

Christopher A. Brown <sup>a,\*</sup>, Hans N. Hansen (1)<sup>b</sup>, Xiang Jane Jiang (1)<sup>c</sup>, François Blateyron (3)<sup>d</sup>,  
Johan Berglund (3)<sup>e,f</sup>, Nicola Senin <sup>g,h</sup>, Tomasz Bartkowiak <sup>i</sup>, Barnali Dixon <sup>j</sup>,  
Gaëtan Le Goïc <sup>k</sup>, Yann Quinsat <sup>l</sup>, W. James Stemp <sup>m</sup>, Mary Kathryn Thompson (3)<sup>n</sup>,  
Peter S. Ungar <sup>o</sup>, E. Hassan Zahouani <sup>p</sup>

<sup>a</sup> Worcester Polytechnic Institute, USA

<sup>b</sup> Technical University of Denmark, Denmark

<sup>c</sup> University of Huddersfield, UK

<sup>d</sup> Digital Surf, France

<sup>e</sup> Sverea IVF, Sweden

<sup>f</sup> Chalmers University of Technology, Sweden

<sup>g</sup> University of Nottingham, UK

<sup>h</sup> University of Perugia, Italy

<sup>i</sup> Poznan University of Technology, Poland

<sup>j</sup> University of South Florida, USA

<sup>k</sup> Le2i, Université de Bourgogne, France

<sup>l</sup> LURPA, ENS Paris Saclay, France

<sup>m</sup> Keene State College, USA

<sup>n</sup> GE Additive, USA

<sup>o</sup> University of Arkansas, USA

<sup>p</sup> Ecole Nationale d'Ingénieurs de Saint-Etienne, LTDS, France

## ARTICLE INFO

**Keywords:**  
Surface  
Metrology  
Roughness

## ABSTRACT

This work studies multiscale analyses and characterizations of surface topographies from the engineering and scientific literature with an emphasis on production engineering research and design. It highlights methods that provide strong correlations between topographies and performance or topographies and processes, and methods that can confidently discriminate topographies that were processed or that perform differently. These methods have commonalities in geometric characterizations at certain scales, which are observable with statistics and measurements. It also develops a semantic and theoretical framework and proposes a new system for organizing and designating multiscale analyses. Finally, future possibilities for multiscale analyses are discussed.

© 2018 Published by Elsevier Ltd on behalf of CIRP.

## 1. Introduction

Surfaces cover everything. Heat, mass, loads, and charge transfer across surfaces. Contact, wear and adhesion occur between surfaces. Cracks and degradation start at surfaces. Surfaces scatter, reflect, and absorb radiation. Wetting occurs on surfaces. These and other topographically related phenomena are considered.

Surface topographies influence many things, and almost all manufacturing processes influence surface topographies. Physical features of different sizes comprise topographies. These will often appear to be different when observed at different scales of observation, hence the need for multiscale considerations. An impressively comprehensive overview of surface generation, surface characterization, and surface function can be found in Whitehouse [189].

The study of surfaces has a long tradition within CIRP. The Scientific Technical Committee – Surfaces deals with research into the geometrical, physical, and chemical properties of the workpiece surface in relation to the production process. A number of excellent keynote papers have been produced throughout the years on the characterization of surfaces. In 2000 De Chiffre et al. gave an overview of characterization methods for surfaces, including 3D roughness parameters [64]. Three years later surface technologies related to micro and nanotechnology were presented, including discussions on characterization [63]. In 2008, Bruzzone et al. presented relationships between surface characteristics and their functional performance [48].

However, these excellent studies predate much of the work on multiscale analyses. Despite all the work on topographies, there is still a lack of experimental evidence of correlations or discrimination for many situations in which surface topographies are suspected of being involved. This is despite the multitudes of parameters available for characterization [4,60,83]. Traditional parameters appear to lack systemization [60,188] and can seem

\* Corresponding author.  
E-mail address: [brown@wpi.edu](mailto:brown@wpi.edu) (A. Brown).

disconnected from each other and from design and manufacturing applications. It is also often unclear which parameters might be useful for a given situation [60]. Publications that suggest parameters for specific applications should cite experimental evidence with functional correlations for validation.

Here, the term multiscale analysis describes the process of studying topographies at multiple scales of observation, and comparing, merging, or associating the findings, acquired from observations or calculations at different scales. Conventionally, measured topographies are decomposed into a small number of scale ranges, e.g., roughness, waviness, and form [4], which are not sufficient to solve many of the problems addressed here. To be included in the discussions in this work multiscale analyses and characterizations must be applied intentionally, systematically, and in detail over a significant range of scales.

The results of multiscale analyses have the potential to add value and reduce costs in the design of products and processes. Multiscale analyses facilitate the understanding of relations between processing or performance and topographies. Multiscale analyses also can elucidate certain fundamental scales for surface interactions in physics, chemistry, and biology, and advance the understanding of many topographically related phenomena. Scale ranges from atomic to cosmic can be interesting.

### 1.1. Objectives

The objective of this work is to review multiscale analyses and characterizations of surface topographies, to discuss future possibilities and to synthesize a system for the organization and designation of multiscale analyses. Methods, applications, and associated insights are included, for a wide range of applications. Analyses and characterizations with potential that help solve manufacturing, tooling, quality assurance and process design problems are of particular interest. However, multiscale analyses and characterizations are also valuable for addressing scientific questions involving topographies in other fields, such as, geography, paleontology, and archaeology. In addition, the multiscale characterizations and analyses developed by researchers in these fields can be valuable when applied to industrial problems. Thus, a review of multiscale analyses and characterizations in the scientific literature is also included where appropriate.

Section 2 provides definitions of terms and concepts. Sections 3 and 4 review engineering and other multiscale applications. Section 5 provides a systematic synopsis of the methods. Section 6 includes syntheses and concluding remarks. Table 1 defines less common abbreviations that appear here in multiple, non-sequential paragraphs.

**Table 1**  
Abbreviations particular to this study.

SI	Sampling interval – the spacing between measured heights reported in a measurement
SZ	Sampling width – the region over which a measured height is determined by the instrument
FD	Fractal dimension
CP	Characterization parameter – a metric that describes the topography
MC	Multiscale characterization – CPs that describe an aspect of the topography as a function of scale
MCSS	MC statistical summary – a characterization that summarizes the MCs that vary with position
MAC	Multiscale analysis for characterization – analysis done in order to calculate the values of MCs
MSA	Multiscale statistical analysis – analysis completed for correlation and discrimination based on MCs

## 2. Definitions and concepts

This section begins with basic terminology to build a semantic and theoretical framework for studying multiscale phenomena and advancing surface metrology as a scientific discipline.

Surfaces are thin, continuous regions that define a boundary in composition or phase. Abrupt physical and chemical gradients, that are normal to surfaces, define the boundaries of these regions. Topographies are collections of locations of surfaces.

### 2.1. Scales

The term “scale” has had many meanings in metrological studies. Scale can refer to the ratio of lengths on measurement renderings to the actual lengths on the actual surface. In this paper, and in much of the literature, scale refers to a segment of wavelengths or spatial frequencies. This segment, range or window, can be narrow when compared to the full size of a measurement. When scale is used without a modifier or with a single value, this segment is intended to be as small as the sensitivity in the measurement, be it linear, areal, or volumetric.

The concept of scale is often enmeshed with size. Topographic features of a given size will be best discernible when observed at certain scales. Thus, scale and size are often used interchangeably.

Scales are important. Topographically dependent behavior can be controlled by physical interactions taking place at multiple scales. Topographic modifications during fabrication or use (e.g., wear) can occur at multiple scales. The ability to understand the relationships between surface topographies and the phenomena that influence them, during manufacturing and use, depends on how topographies are measured, analyzed, and characterized at multiple scales. The scales that are useful for understanding interactions with topographies are generally not known *a priori*.

Strong functional correlations and confident discriminations are important for understanding how topographies should be specified to optimize products and manufacturing processes. These understandings can lead to better product and process designs and improved quality assurance and quality control.

Knowing the scales of interactions for topographically related phenomena is important. Many engineering surfaces must fulfil multiple functions that can require different kinds of topographies.

In certain situations, different functions can be adjusted by different topographic characteristics on the same surface. The different characteristics that control these functions can coexist on the same surface, at different scales. For example, road surfaces should be smooth at larger scales for a comfortable ride, and rough at finer scales, to provide friction for turning and stopping.

A systematic approach to solving these kinds of topographic design problems would involve determining the scales of the different interactions controlling the functions. The scales of these interactions could be determined by using multiscale analyses and characterizations appropriately.

### 2.2. Roughness and irregularity

Mandelbrot [117] titled the introduction to his autobiography ‘Beauty and Roughness.’ He noted that common patterns in nature are nearly all rough, having exquisitely irregular and fragmented aspects to them. The omnipresence of irregular roughness, its multiscale nature, and its complex influence on functionality are not always adequately considered, even in supposedly sophisticated experimental work.

Real, manufactured surface topographies tend to be irregularly rough at sufficiently fine scales. Many developments in manufacturing can be seen as efforts to push irregular roughness, and its inherent geometric uncertainty, to finer and finer scales. This irregularity can make the characterization of topographies particularly challenging. The values of geometric topographic characterization parameters (CPs) depend on the scales of the measurements and of the calculations in their computations. It could be that only a few of these scales are useful for understanding a particular topographically related phenomenon.

On irregularly rough surfaces, fundamental geometric properties, like area and curvature, change with scale. The appropriate scales for analyzing areas for heat or mass transfer, or for analyzing

slopes for scattering, or for analyzing curvatures for calculating stress concentrations that influence fracture, can be determined through appropriate experimental design and the use of multiscale analyses and characterizations.

### 2.3. The nature of topographic measurements and their scales

The measurement is not the surface, just as a painting is not the object painted [112]. The knowledge of the topography of irregularly rough surfaces is always incomplete. Scales in measurements and their influence on subsequent analyses and characterizations are occasionally overlooked. This section addresses these oversights and provides part of the basis for a discussion of multiscale analyses and characterizations.

Regardless of how many heights that are known and at however many locations, the height at any other location on an irregular surface can only be estimated. This is in contrast to mathematical models of smooth, regular shapes, where all positions on the surfaces are known exactly.

The nature of topographic datasets created by a measurement instrument also plays a fundamental role in determining what feature sizes can be observed. Profile data ( $z = z(x)$ ) and areal data ( $z = z(x,y)$ ) are typically returned from current state-of-the-art measurement instruments. In both cases, height sample data ( $z$ ) are referred to specific,  $x$  or  $x,y$  locations, at equally spaced sampling intervals (SIs) on a regular grid. For areal datasets, heights are typically organized as a matrix of values (equivalent to a digital, intensity image), where the sampling interval (SI) is equivalent to pixel size or width. Triangulated meshes are also possible, especially from industrial computed tomography, but they are typically converted into  $z = z(x,y)$  format by virtual raster scanning.

SIs are the smallest spatial component of the uncertainty, or resolution. The smallest regular wavelength detectable, from the Nyquist criterion would be half the SI. A distinction is made here between the pixel width in images rendered from measurements, and the resolution of the sensor in the measurement instrument. The sensor samples heights over a sampling zone (SZ) with a finite size. One height is reported at each location, although heights might vary within the SZ. The SZ limits the lower resolution of an instrument. The actual width of the SZ is rarely known, nor is the function that calculates the one height reported for that SZ.

The SI (pixel size), and the number of rows and columns in the matrix of height values (the number of pixels), determine the range of observable sizes, or scales, in a measurement. Despite claims in the literature of subpixel or subvoxel resolution, multiscale characterizations do not vary significantly below the sampling interval in the measurement [132].

In multiscale analysis, multiple observational scales are applied to the same topography. This could be implemented through the use of multiple measurement instruments, multiple setups of the same instrument, e.g., optics with different magnifications, or even through multiple data processing paths applied to the same dataset, as long as they are aimed at extracting different, scale limited content. In all cases, it is possible to investigate the surface using complementary or partially overlapping scales. For example, a surface might be measured at  $5\times$ ,  $10\times$ , and  $20\times$  magnification. Many features could be present across two or more of these measurements, although they might appear differently at different magnifications. In the case of operating from a single dataset, scales are extracted via data processing. An effect similar to measuring at different scales can be approximated by filtering. For profile and areal datasets, size can be mapped to the concept of spatial wavelength or frequency; therefore, filtering by feature size is often implemented through frequency-based filtering.

In summary, measurements cannot completely describe the topography of a surface. Surfaces cannot be detected at infinitesimally small spatial locations. The height at a point cannot be measured, and has little physical meaning in production engineer-

ing. The surface can only be detected, over an SZ with a finite size. When height measurements are said to locate a "point" on the surface, it is a data point, not a physical point. The size of the SZ, which can be a length, areal region, or volume (CT, computed tomography, see Section 3.3 below), contributes to the uncertainty in the measurement. Within the SZ the surface is not perfectly smooth. Therefore, it is impossible to measure or to know all the heights on a measured, irregular surface.

### 2.4. Multiscale analysis for characterization

A characterization parameter (CP) is a metric that describes an aspect of a measured topography. The most widely used CP is Ra, average roughness of a profile [172]. However, any mathematical transformation starting from topographic data and leading to a scalar, vector, or, as in the case of curvature, a second-order tensor [10,103], can be chosen for characterization. In a particular application, a certain CP might be favored because it is expected to be indicative of topographic properties associated with the phenomena of interest.

Multiscale analyses for characterization (MACs) calculate CPs over a range of scales. A multiscale characterization (MC) shows how CPs vary over a range of scales. Multiscale characterization statistical summaries (MCSSs) are used to summarize MCs that vary with position over the surface. MCSSs can emphasize means, extreme values, variance, skew and kurtosis, as do conventional CPs of heights [4].

MACs can operate on a single dataset from one measurement. A single configuration of the measurement system, and a single uncertainty model, provide comparable results over the range of scales in that measurement. Thus, appropriate combinations of filtering, down sampling, resampling, or spatial frequency decomposition of the measurements, e.g., wavelets or bandpass filters, can simulate, or approximate, the effects of measuring at different observational scales [4,36,41,83].

Any type of CP can be calculated and observed across multiple observational scales by appropriate multiscale processing of individual measurement datasets or by multiple measurements. Subsequent analyses can reveal characteristics of the DP, like stability across scales, or significant variations at specific scales.

Area, length, slope, and curvature all change with scale on irregular topographies. These geometric MCs inherently provide clear physical interpretations in certain applications.

New CPs can be defined by combining MCs obtained on the individual datasets. These new CPs are multiscale parameters, or indicators, because they cannot be computed without multiscale analyses (Fig. 2.7.1). A typical example of a multiscale indicator defined from a combination of MCs is the fractal complexity [83].

Discovering or identifying functional correlations is often a matter of solving regression problems involving an observed behavior or performance and one or more MCs. MSA in these cases can assist because it can identify strong correlations with MCs, and identify changes of correlation strength across ranges of scales, hence identifying scale-specific phenomena and behavior.

MSAs can help solve discrimination problems, i.e., identifying which CPs, and at what scales, are the most relevant at telling topographies apart. This can be in relation to other observed differences, e.g., in the functional or manufacturing domains.

Discoveries of the scales of the best correlations and discriminations can be used to advance many kinds of scientific disciplines. This would include the role of topographies in fundamental interactions in physics, chemistry, and biology.

MSAs can also be applied to the evaluation of measurement systems, including instruments, measurement parameters, and replicas, as well as filters. MSAs and MCs can be used to study such things as noise, outliers, and resolution. The best measurement and filtering options could be the one that provides the strongest correlations or the most confident discriminations.

## 2.5. Fractal analyses as multiscale analyses for characterization

There is abundant literature on fractal analysis of topographies. It deserves its own review. For many natural and mathematical shapes, the CP, fractal dimension (FD), should be insensitive to scale, at least over ranges of scales, while crossover scales define scale limits of FDs [116]. The FD generally exceeds the Euclidian dimension and be between 1 and 2 for a profile and between 2 and 3 for a surface. To calculate an FD, a range of scales needs to be considered, therefore, all fractal analyses might be considered MACs. However, to be considered MACs here the FDs must change with respect to scale.

Many surface topographies, including manufactured surfaces, are frequently multifractal with respect to scale. Scale-sensitive fractal analysis (SSFA) FD calculates the FD from the slope of a graph of a geometric property versus scale. When the slope of that graph varies, then the topography is multifractal with respect to scale [4,144]. Characterizing such surfaces with a single FD can result in missing important insights and understandings [204].

Surfaces are often initially conceived of and designed as smooth forms. The smooth form is usually maintained at large scales in the manufactured part. Irregular features, or roughnesses, often exist at sufficiently fine scales. At the scales at which the surface is approximately smooth, then the FD approaches the Euclidian dimension. At a finer scale, surfaces are often rough and the FD clearly exceeds the Euclidian dimension. This scale is the smooth-rough crossover scale [4], which provides a physical definition of roughness, based on the surface itself. Conventional waviness could be included in this fractal-inspired definition of roughness, if the amplitude is large enough and it is sufficiently irregular [40].

## 2.6. Reviews of multiscale analysis or characterization

Although several previous STCS keynotes have included aspects of multiscale topographic analysis, there has not been a comprehensive review with multiscale topographic analysis as the prime focus.

Lonardo et al. [109] dealt with MACs in addressing patchwork, or area-scale, analysis. These have since been included in ASME [4] and ISO [83] standards. Also addressed were other kinds of fractal analyses, although not all of these recognized the multiscale nature of manufactured surfaces.

De Chiffre et al. [64] dealt with MACs, particularly fractals, structure function, area-scale analysis, and wavelets. Different techniques for analyzing fractal surfaces were discussed, such as the structure function and area-scale analysis. Many examples of applications were given. Wavelet transformations, with different implementations and several examples of applications were described at length. The possibility of using wavelet filter banks for multiscale analysis was also demonstrated.

Jiang and Whitehouse [91] dealt with MACs in terms of wavelets, fractals, and area-scale analysis and gave examples of applications for MACs. A description of wavelet theory was given and examples of different implementations were provided. In addition, an example with a multiscale decomposition of a milled surface was presented. Evaluation of fractal geometry is described at length. The difference between a pure fractal surface and a Markov surface was explained. A method for extracting the fractal properties, dimensions, and topography was presented. Area-scale analysis [4,83] was explained in detail. Several examples of the use of MSA methods were given, such as relating the adhesive strength of coatings and friction in sheet metal forming to surface texture.

Malshe et al. [114] gave a review specifically on bioinspired, engineered surfaces. Many examples of functions, such as super hydrophobicity and related multiscale properties were given. Descriptions of design and manufacturing methods were also presented. Quality control or characterization of these surfaces was not discussed.

In a review for the Royal Society in 2007, Jiang et al. dedicated two sections to MACs by means of wavelet transforms and

examined fractal surfaces through geometrical approaches, such as volume-scale and area-scale analysis [89]. They pointed out that the identification of crossover scales, where the fractal characteristics of surface texture changes, can be used for identifying ranges of scales with different dominating textures that influence creation or wear processes.

Although the focus was on scales that are common to product and process design, as mentioned above, other scales were considered. This is because there can be useful insights from analyses and characterizations outside these scales, which could be used to solve engineering product and process design problems.

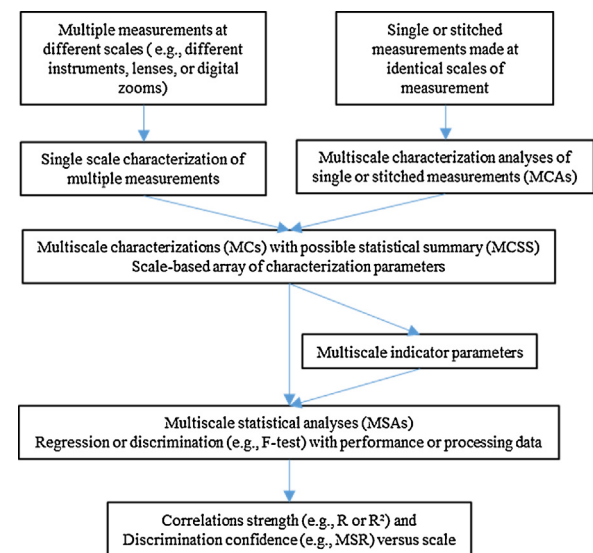


**Fig. 2.7.1.** Multiscale analyses and characterizations: flow and types.

## 2.7. Summary

There are different approaches to certain aspects of multiscale analyses and characterizations. The most common are shown in Fig. 2.7.1. Multiple measurements, at different scales can lead to an MC. More commonly, there is a MAC a single topographic measurement that leads to MCs. These MCs might capture a particular geometrical aspect of the surface that could be applicable to a situation, like positive curvatures for stress concentrations in fracture [184]. A few of the papers stop there, with the presentation of potentially valuable information about a characterization method. When the MCs vary with position over the surface, such as with curvature, then appropriate MCSSs can be used to represent the MCs. Papers have gone on to perform MSAs to study the strength of correlations with phenomena of interest [184], or to discriminate surfaces that were processed or that perform differently [93]. Multiscale analyses can use conventional height or hybrid parameters when they are applied after a decomposition by spatial frequencies as discussed below in Sections 5.2 and 5.3, on wavelets and sliding bandpass filters.

## 3. Engineering applications

### 3.1. Conventional manufacturing processes

Understanding quantitatively how manufacturing processes modify topographies in different ways is essential for process design. Topography characterization can be a useful tool for analyzing effects of manufacturing processes during process development or tuning process variables. Many surfaces are manufactured using a series of sequential processes, or process variations, to reach the final finish. Employing a multiscale

approach can be an efficient way to characterize such surfaces, since every process leaves its own topographic signature. The discovery of reliable, quantitative, functional correlations between the processes and variables and the resulting topographies can be facilitated by MSA.

Boryczko [28] studied profiles on turned surfaces using power spectral density (PSD) to look at irregularity in the profile inside the roughness, waviness, and form and found that the cumulative amplitude spectrum can provide knowledge about a machine tool's capabilities, accuracy, and wear.

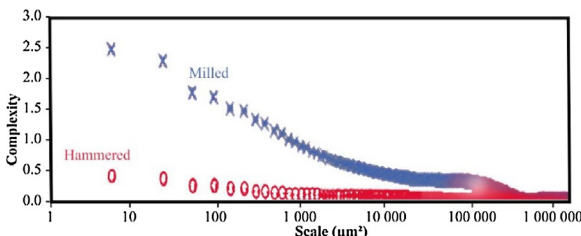


**Fig. 3.1.1.** Complexity calculated at 471 scales after milling and subsequent hammering. Mean values of five measurements with 95% confidence intervals [19].

In Berglund et al. [19], the effect of a novel finish machining process was characterized, using area-scale analysis among several other methods. The examined workpiece was made of nodular cast iron, and the surface was first finish milled, using a ball-nose end-mill, and subsequently processed by machine hammer peening. Using ISO 25178 height parameters, the effect of the hammering was apparent: the overall height of the topography was dramatically reduced. However, using area-scale analysis (MCs relative area and complexity as functions of scale), the effect could be studied in more detail (Fig. 3.1.1). Topographic changes in the scales of milling cutting data could be distinguished from changes in the scales of the nodules and fine scale roughness with statistical significance using confidence intervals, thus providing an MSA.

Bigerelle et al. [23] used MSA to study the ability to discriminate the roughness of surfaces made by injection molding as a function of four process parameters. The MAC used conventional height parameters evaluated as a function of evaluation length and the degree of polynomial fit for measured profiles. The experiment was designed to find the most relevant roughness parameters, the most pertinent scale, and the degree of polynomial fitting. Their 'pertinence' is shown versus scale in Fig. 3.1.2. When the measured profiles are fit with first or second degree polynomials, there is a narrow range of scales where the pertinence reaches a distinct maximum. The method allowed the determination of the most efficient combination of parameter, degree of polynomial fit, and scale for discrimination of the process variables, and for the determination of the scale at which each process modifies the roughness.

Bruzzone et al. showed in 2004 [206] that wavelets, previously used for analysis, compression and filtering in signal processing, provide a powerful multiscale representation of machined surfaces. Later, the surfaces of machined natural fiber composites were characterized with MAC and MCs, using wavelets and the multiscale process signature, which is the ratio of the change in roughness after milling to the initial roughness as a function of scale [57]. Three scale regions were noted, corresponding to the fibers, bundles of fibers, and global. The contribution of fiber stiffness and feed differs with scale and behaviors specific to the characteristic zones. The results demonstrated that MSA shows that the machined surface topography relates to the mechanical behavior. Liu et al. [108] also used wavelets to show that on ball-end milled surfaces measured with an optical profiler, at high spatial frequencies, the surface micro roughness increases with the increasing spindle speeds, whereas at low frequencies the waviness of surfaces machined at high spindle speed is small.

A large number of manufacturing processes, including rolling, fine machining, and selected abrasive finishing, were examined in the context of determining the relative abilities of MSA using bandpass filtering with three different kinds of filters [100]. Conventional height parameter applied to the bandpass-filtered measurements were compared for the ability to discriminate topographies resulting from different processing. The relevance of the parameters, i.e., wavelets, Gaussian, and discrete modal decompositions, was found to depend on the nature of the surfaces examined.

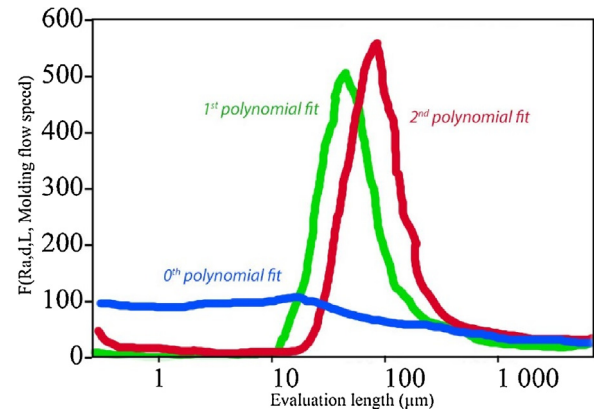


**Fig. 3.1.2.** Pertinence versus evaluation length (scale) where the degree of polynomial fit used on the measured profiles is indicated as d, L is the evaluation length and Ra is the average roughness [23].

Surfaces created by machining, including conventional, abrasive, and EDM, have been described with the MCs length-scale [4,61,44,40,42,166] and area-scale [4,83,166,202,93,82]. These methods are suggested by fractal geometry, originally demonstrated by calculating the lengths of coastlines as a function of scale [116]. This coastline, or length-scale analysis, can separate the regular component of turned surfaces at larger scales, confidently identifying the feed per revolution, from the irregular components at finer scales, as shown in the length-scale plot of a turned surface profile in Fig. 3.1.3. The relative lengths and relative areas as a function of scale are the MCs. MSA using area-scale has been shown to be capable of discriminating grinding conditions and scale ranges where they differ, and using length-scale for showing the grinding direction, on polyethylene ski bases, textured for sliding on snow [93].

MACs were done on 3D roughness measurements made with a contact stylus (tip radius ~2 μm) to study the influence of abrasive size on stainless steel surfaces polished with different grit abrasive papers. Extreme Amplitude of Peaks to Valleys (EAPV) versus the scale of observation were used for MCs. The geometrical characterization was selected for applications where highest peaks or valleys are critical parameters, which would be the case for surface integrity, e.g., crack initiation, for predicting product life. Three abrasion regimes could be identified. First, for abrasive particle size greater than 125 μm, the EAPV and wear rates of the stainless steel workpiece were high. Then, when the abrasive was between 10 μm and 125 μm, the EAPV diminished with the grain size at all scales, comprising the grit size effect. Finally, when the grain size was less than 10 μm, the EAPV decreases dramatically at all scales and was insensitive to the size of the particle. This has proved useful for studying manufacturing and abrasive wear phenomena [21].

Bartkowiak and Brown [10] used multiscale curvature tensor analysis to study conventionally machined and, subsequently, ground steel surfaces. MSA indicated the transitions in natures of the topographies due to the finishing. They found that the distribution of principal curvatures (an MCSS) was altered during grinding of a machined surface. Both maximum and minimum principal curvature values decreased after abrasive processing. At the finer scales, ground surfaces tended to be more curved than the

milled surfaces. This was explained by the fact that the geometry of the abrasive for grinding is more varied than the nose of the cutting. The ground surfaces are flatter, whereas milled surfaces reflect the geometry created by feed and the nose tool.

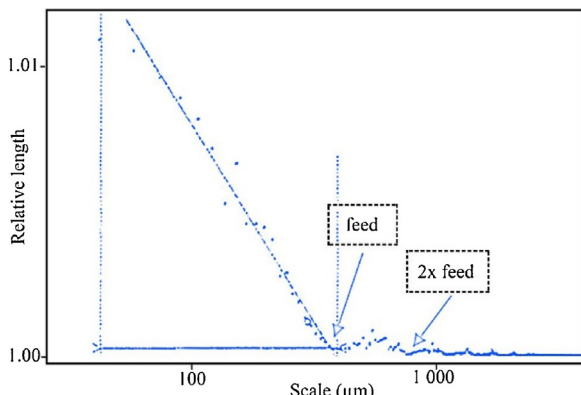


**Fig. 3.1.3.** Relative length versus scale plot for a surface turned with a feed of 0.5 mm/rev [42].

For surfaces created by micro EDM (electric discharge machining) Hyde et al. [82] found correlations as high as  $R^2 = 0.99$ , between discharge energy and the relative areas, area-scale complexities, and the SRC [4,83]. The scales of the strongest correlation were between 10 and 200  $\mu\text{m}^2$ , scales corresponding to a few of the largest discharge craters. The MAC for curvature tensors applied to the same surface measurements showed that there existed strong correlations between discharge energies and the statistical curvature parameters: mean principal curvature  $\kappa_1$ ,  $\kappa_2$  and mean curvature H for scales between 1 and 100  $\mu\text{m}$  [10]. Gaussian curvature K, an MCSS, appeared to correlate the strongest for the widest range of scales. It was found that an MCSS using combined average and standard deviation of curvature parameters also strongly correlates when an MSA regression is used with discharge energy:  $R^2 > 0.99$  at 3.125  $\mu\text{m}$ . For the machined and ground surfaces at finer scales, ground surfaces tended to be more curved than the milled surfaces, while the opposite tends to be true at the larger scales.

To compare simulations of the formation of conventional machined surface topographies, the MCs, area-scale and complexity scale [4,83] were also used by Lavernhe et al. [99]. One assumed the tool nose to be smooth; the other included a measured tool nose profile. These MCs showed the scale limits of the simulations compared to the actual machined surface.

The MC relative area was used to study the surface topographies, of pharmaceutical excipient compacts with different compositions and particle sizes measured with an interferometric microscope. The MCs relative area and complexity [4,83] could discriminate according to a MSA f-test below scales of about 1000  $\mu\text{m}^2$ . Strong correlations from linear regression MSA, with breadth of particle size distributions ( $R > 0.99$ ) were found at 10  $\mu\text{m}^2$ . Conventional parameters were not able to discriminate or to find correlations. The multiscale analysis and characterization provided a basis for a better phenomenological understanding of behavior for the prediction of mechanical properties from surface measurements [125].

Optical surfaces created by precision milling and single-point diamond turning of crystals were measured by AFM and studied with a combination of fractal and wavelet analysis. The high frequency components of the machined surfaces topographies can be independent of the machining process, reflecting anisotropic aspects of the workpiece material. The wavelet decomposition showed distinct, scale-dependent features from the two kinds of machining [58].

Wavelets are also used on surfaces made by abrasive belt finishing and measured with a white light interferometer [123]. A

multiscale decomposition for MAC was based on a continuous wavelet transform, which provided the multiscale transfer function of the surface topography by the finishing process. The ranking of the transfer function with respect to grit size varied with scale. Belt finished surfaces with different processing were successfully discriminated, and the topography was understood in the context of the physics and tribological mechanisms of the process.

### 3.2. Additive manufacturing

Multiscale methods are important for surfaces made by additive manufacturing (AM). Conventional CPs were developed primarily for characterizing surfaces created by machining and abrasive processing; AM probably requires different CPs. In MC of AM surfaces, many characteristics can be found that are similar to those in conventional manufacturing. MAC can show that both kinds of surfaces can have regularity at the scales of the programmed toolpath. These scales are generally below the scales of the form and above those scales where the material composition interacts with the manufacturing process, resulting in irregular features, and these scales are revealed by many kinds of MC.

The scales influenced by the tool path and material response to post deposition processing on an FDM (fused deposition modeling) surface are shown in Fig. 3.2.1. MC by relative length versus scale can show patterns similar to those found on turned surfaces. The lobes where the material is deposited in tubes is nearly the mirror image of grooves where material is scraped out by the tool nose.

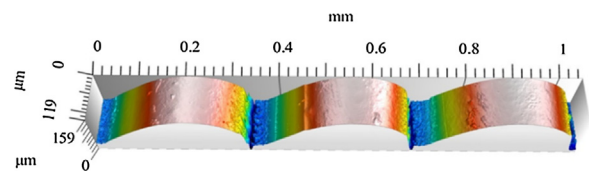


**Fig. 3.2.1.** Rendering of a measurement made by a scanning laser confocal microscope of a surface by fused deposition modeling: layer thickness 254  $\mu\text{m}$ , bevel angle 45° modified to reveal 359  $\mu\text{m}$  [200].

Fig. 3.2.2 shows MSA by an F-test discriminating layer thickness by the MC area-scale complexity [4,83]. The plot of mean square ratio versus scale shows that this MC discriminability with at least 99.9% confidence between areal scales of 0.3 and 25  $\mu\text{m}$  and, at the finer scales, below 0.3  $\mu\text{m}^2$ , in the scale range where it should be expected that the surface topographies are more a function of the material response to the process. In this scale range, the differences diminish between the layers' complexity, due to the toolpath that facilitated the discrimination at larger scales. The diminished ability to discriminate at scales below 0.3  $\mu\text{m}^2$  should not be surprising because the materials and their reaction to the process are similar, and their topographies become more similar at finer scales. Additionally, these fine scales could be approaching the limits of the instrument.

Deposition angle by FDM of ABS and subsequent polishing with acetone vapor were studied by Brown et al. [37,38], using the MCs relative areas and area-scale complexities. Scales of pillar-like defects, apparently part of the material reaction to the deposition process, were identified. Surfaces were discriminated at the scale of the deposition layer thickness and at finer scales more than twice as often by multiscale than conventional analyses [37,38]. In Bartkowiak et al. [13], a multiscale curvature tensor analysis was used to characterize the same surface textures of FDM parts, which were subsequently treated with acetone. The plots of curvature versus position at different scales showed things about the character of the differences between surfaces, which are not evident from conventional height or hybrid parameters. The latter, calculated at specific scales, miss the transitions in the natures of the topographies that are evident in the curvature MCs.

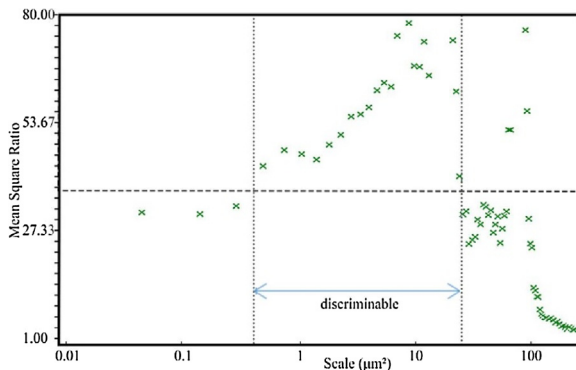


**Fig. 3.2.2.** MSA for discrimination (F-test), with 99.9% confidence, between complexities for 254 versus 330  $\mu\text{m}$  layers on a 45° FDM bevel [200].

In laser sintering of powders, topographies show defects of incompletely fused powders, which can cause outliers in confocal measurements [50]. Outlier filtering shows that large-scale modifications influence the MCs, relative areas, at smaller scales, but not the complexities [83,50].

In laser sintering of powders, the process parameter of linear energy density used in sintering was found to correlate well with MCs, relative areas, ( $R^2 > 0.99$ ) and area-scale complexity ( $R^2 > 0.95$ ) using the MSA linear regression [104]. There are many poorly sintered powder particles on these surfaces, which tend to introduce outliers in the measurements. Several methods were attempted to remove the outliers. Interestingly the best correlations were found doing the MSA with the unfiltered data.

### 3.3. Computed tomography

X-ray CT is a nondestructive imaging technique that is increasingly used for dimensional metrology [98]. It is used for multiscale analyses in several industrial sectors [62]. To perform MSA like other current measurement methods, resolution is an issue, as are dealing with more than one height at a spatial location, distinguishing the surface pixels, and establishing a datum for pores and full objects. These are among the most important future challenges for surface metrology.

Typical cone-beam CT scanners are capable of characterizing surfaces at different scales of observations, depending on the magnification factor used. Besides magnification, several other factors influence the resolution and accuracy of CT measurements [55,73,54,107,192]. Recently, CT has started to be considered as an effective technique for topography measurements at microscale, especially for internal and difficult-to-access surfaces and mainly in the case of parts with high surface roughness such as additively manufactured (AM) parts [170]. High surface roughness is a major cause of deviations between dimensional measurements performed with different techniques, such as tactile coordinate measuring machines, optical systems, and CT [56]. Recent works have studied the influence of surface roughness on CT dimensional measurements, investigating the combined effect of surface morphology and CT measurement characteristics [2,107].

Multiscale analysis has great potential to contribute to AM part and process inspection and design. CT is required for inspecting internal surfaces in additive manufacturing (AM) [15,62,186]. These can have multifunctional, 3D internal lattices and trusses [171]. CT measurements of AM parts blur the boundary between form and topography.

Surface identification is an issue in interpreting CT data [173,174]. Surface topography can be estimated from volumetric CT data to a certain scale, depending on the material and the part. Townsend et al. claim an order of magnitude of subvoxel uncertainty in the scale of the resolution for determining surface parameters. Researchers have studied the surface in sections, as with Lou et al. [111], who applied conventional parameters to full CT surface measurements, using a triangular mesh and diffusion

equations for filtering. This method might have unrealized opportunities for MAC, through variation of the triangle size in the mesh and the parameters in the filtering.

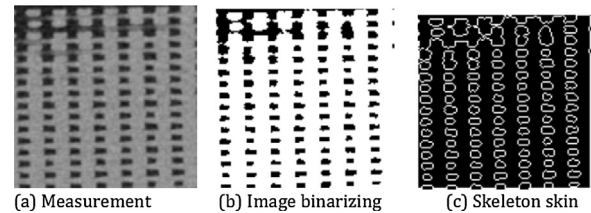


**Fig. 3.3.1.** Surface extraction from the CT measurement shown in a cross section [132].

A multiscale approach for the analysis of the internal part geometry from CT measurements is proposed in Quinsat et al. [132]. It is based on an MAC to determine the MC 'relative internal area'. This applies to the surfaces of all the internal structures (no external surfaces). The boundaries, or skin of the structural elements, were determined from the three dimensional, binarized measurement as shown in Fig. 3.3.1. Unlike most current topographic datasets, these include multiple height values at each spatial position. The relative surface area is computed from a variable voxel size, which is manipulated to adjust the scale for the MAC. The variable voxel size can be smaller (subvoxel) or larger (megavoxel) than the initial, measured voxel size. The smallest voxel sizes, below the finest scale of the measurement, are obtained by a linear interpolation between the measured voxels. An internal area could be calculated according to the sum of all the areas of the skin voxel faces:

$$A = \sum_{i=V_{skin}}^6 \sum_{j=1}^6 A_{i,j} \cdot \delta_{i,j} \quad (3.3.1)$$

$$\begin{cases} \delta_{i,j} = 1, & \text{if face } j \text{ belongs to voxel } i \text{ contacting air} \\ \delta_{i,j} = 0, & \text{if face } j \text{ belongs to voxel } i \text{ not contacting air} \end{cases}$$

This area depends on the volume included in the analysis and is normalized to determine the relative internal area  $A_r$  by dividing the bounding voxel area  $A_b$  so that  $A_r = A/A_b$  (Fig. 3.3.1(a)). The relative internal area increases with decreasing size of the megavoxels, to a plateau (Fig. 3.3.2). This plateau starts close to the scale of the cross sectional area of the measured voxels ( $37.8 \times 37.8 \mu\text{m}^2$ ) and extends through the sub-voxel scales, showing that the sub-voxel interpolation does not provide any new knowledge about the surface with this MP. The MAC is applied to the CT measurements of three specimens, with different filling modes. Results show that the evolution of relative internal area depends on the filling mode (Fig. 3.3.2). These are most distinctly different at the lowest scales.

### 3.4. Adhesion

Conceptually, it can be interesting to imagine a discrete interaction model for topographically related phenomena, like adhesion. In this model, topographic interactions that are often thought of as being continuous can be thought of as being the result of the sum of a large number of discrete interactions on a sufficiently small scale. This is the approach taken by Brown and Siegmann [46] in analyzing the influence of topography on adhesive strength. Therefore, it follows that macroscopic adhesive strength should be the sum of the strength of a finite number of discrete, adhesive bonds.

In Brown and Siegmann [46], a number of substrates with different topographies were prepared by grit blasting. These surfaces were measured by scanning with an instrument using a contact stylus with a spherical tip with a radius of 5  $\mu\text{m}$ . The relative areas were calculated as a function of scale. To do this, first the apparent area was estimated in three dimensions as a function of scale, by repeated virtual tiling exercises with triangles. Starting with triangles half the

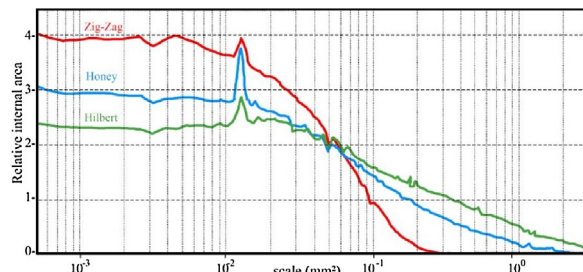


**Fig. 3.3.2.** Filling mode comparison using multiscale analysis [132].

size of the measured region, each repetition used progressively smaller triangles until an area equal to half the square of the SI was reached. The area of the tiling triangle represented the scale of the characterization. Then, the relative areas were calculated by taking the ratio of the estimated area from the tiling exercises to the projected or nominal area, in two dimensions, of the surface covered by the virtual tiling in three dimensions. A coating was applied by thermal spray, and the adhesive strength was measured in straight pull testing. Then, the adhesive strengths were regressed versus the relative areas over the range of scales of this multiscale topographic characterization. Following this, the Pearson correlation coefficients,  $R^2$ , were plotted versus scale. At the large scales, the coefficients were small, less than 0.1. They increased steadily to about 0.9 at about  $75 \mu\text{m}^2$ , remaining approximately constant at finer scales. This is one of the highest correlation coefficients ever reported for relating a measure of the adhesive strength to a topographic characterization parameter. It was noted that this scale is about that of the contact area of the stylus used in the measurement. This result indicates that the scale of the discrete interaction, i.e., fundamental scale for the kind of adhesion in this experiment, is at or below about  $75 \mu\text{m}^2$ . At scales above the fundamental scale, perhaps the model underestimates the adhesive strength, and at scales below the fundamental scale, the adhesive strength might be overestimated, resulting in lower values for the correlation coefficients at these scales.

In a biological application of adhesion, Emerson et al. [70] also used relative area as the MC and regression analyses for the MSA to study bacterial adhesion on rough surfaces using an AFM. They found low, negative correlations with relative areas ( $R^2 < 0.4$ ), suggesting perhaps a lotus effect. The trend of the regression was smooth and showed a minimum of about zero at  $100 \text{ nm}^2$ . The existence of three relative minima suggested that several mechanisms could be active.

In another biological application of adhesion, Bigerelle et al. [22] studied the adhesion of human osteoblasts on titanium substrates. These substrates were textured by EDM to produce 22 different surfaces, which were then coated with a polyelectrolyte, so that surface compositions would be identical. Topographies were measured with a contact profiler stylus with a  $2 \mu\text{m}$  tip. The MAC varied the evaluation length and calculated standard CPs. They determined that the most relevant MC by this method was peak spacing (Sm) and that the best scale of observation was a few times the size of the osteoblasts, about  $400 \mu\text{m}$ . The least adhesion was observed when the peak spacing was about the size of the osteoblasts.

### 3.5. Tribology

The transmission of tangential loads between surfaces as a function of the normal load and the wear of sliding surfaces must depend, at least in part, on the topography of the surfaces. Apparently, the nature of the geometrical characterization and the scale of that characterization can be important in finding strong relations between topographies and tribological phenomena.

In Berglund et al. [17,18], friction in sheet metal forming was evaluated using a bending under tension (BUT) test, and tools with two different surface finishes (fine and rough), and in three different

materials, two tool steels and one nodular cast iron. The surfaces were manufactured using finish milling, with two different cutting conditions, and all had lay parallel to the sliding direction. Topography characterization was made, using ISO 25178 parameters as well as relative area and complexity as functions of scale. Linear regression coefficients ( $R^2$ ) between the friction and (nonMCs) texture characterization parameters were calculated. None of the height, spacing, material volume, void, or segmentation parameters showed good correlations. Strong correlations (nonMSAs,  $R^2 > 0.7$ ) were found with Sdr (developed area) and Sdq (rms surface gradient), which are highly correlated with each other ( $R^2 > 0.9$ ) and most sensitive to the finest scales in the measurement. For area-scale fractal complexity (MCs), the correlation increased markedly at scales below  $200 \text{ mm}^2$ , with a distinct maximum  $R^2$  of 0.9 at  $50 \text{ mm}^2$  (MSAs) as shown in Fig. 3.5.1.

Bandpass filtering, adjusting bandwidth and central frequency (MAC), showed that, after filtering, many of the conventional parameters (MCs), notably the conventional height parameters, correlate well with friction (MSAs,  $R^2 > 0.9$ ), with narrow bandwidths at the finest scales. More recently, Bartkowiak et al. [9] used MAC of curvature tensors on the same measurements and found strong correlations with the friction ( $R^2 > 0.85$  at about  $5 \mu\text{m}$ ) for the standard deviations for all four curvature measures (MCSSs: maximal, minimal, mean, and Gaussian) at certain scales. These results suggest that the frictional responses of surfaces could be related to the variance of their topographic curvatures. In Bartkowiak and Staniak [14] the same approach was used to characterize interactions between machined surfaces during contact with a ruby spherical probe. Strong correlations ( $R^2 > 0.9$ ) between mean and standard deviation of the MCSS maximum principal curvatures and average friction coefficients were found.

In Rosén et al. [133], the structure function was used for multiscale analysis of wear of cylinder bores. By calculating the structure function at different scales (MC), it was possible to draw conclusions regarding the manufacturing conditions, and abrasive media and to identify the amount of wear, and at which scales it had occurred during an engine test.

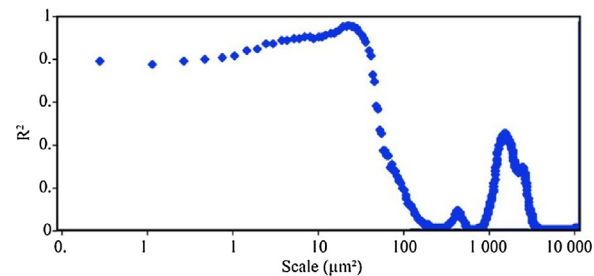


**Fig. 3.5.1.** Correlation coefficient,  $R^2$ , for the correlations between complexity and friction at 587 scales [17,18].

Kennedy et al. [96] showed that static and low-speed friction (stiction) between read-write heads and textured hard discs corresponds inversely to the smooth-rough crossover and the area-scale complexity calculated from AFM measurements. Capillary adhesion is present on these textured glass surfaces, as indicated by tangential force increasing with humidity.

In a geological application based on consideration of transfer of loads across an interface with partial sticking and elastic contact, the evolution of the contact area as a function of scale was used to understand the influence of topography on roughness. At a sufficiently fine scale, the contact area becomes multifractal with respect to scale and provides insight for energy dissipation and the amount of stick across the interface [27].

### 3.6. Fatigue and fracture

It is well accepted that topography has an influence on the fatigue limit and that the size of the influential surface features

depends on the material. Nonetheless, strong correlations between CPs and fatigue limits are not generally demonstrated in the literature with explicit regression analyses of CPs calculated from topographic measurements.

MC by curvature, using Heron's formula [76], on profiles extracted from areal measurements parallel to the tensile stress, was applied to steel surfaces machined by ball-end milling with different conditions [184]. Over a narrow range of scales, MSA by linear regression showed that the fatigue limit correlated strongly ( $R^2 > 0.96$ ) with the MCSS mean of the curvature, plus two standard deviations. Specimens heat-treated to relieve residual stress induced by machining were included in the analysis and fell close to the regression line (Fig. 3.6.1).

Surface features or defects are thought to provide stress concentrations that can lead to fracture. Narayan et al. [125] found strong correlations between relative areas (MCs), and the brittle fracture index ( $R^2 > 0.7$ ) over a wide range of scales, while the tensile strength was favored over more specific scale ranges.

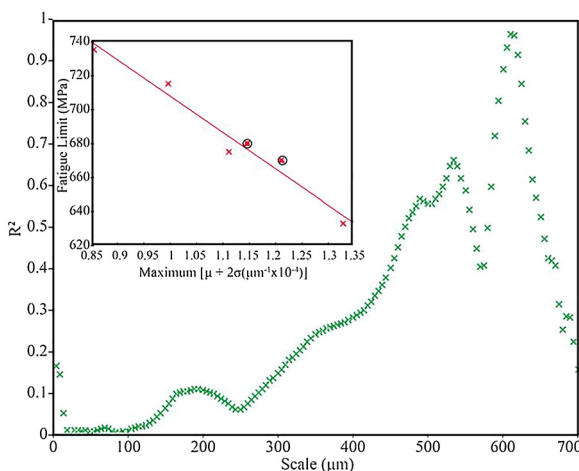


**Fig. 3.6.1.** MSA for the coefficient of the MSA linear regression versus the MCSS mean of the curvatures, plus two standard deviations versus the fatigue limit, plotted versus scale. The insert shows the regression at a scale of 610  $\mu\text{m}$ . The two results that are circled on the insert were from specimens that were not heat-treated [184].

### 3.7. Outlier filtering

Surface measurement instruments can acquire large datasets quickly, although occasionally with aberrant height samples, which are outliers. Outliers can distort CPs, mask functional relations, and adversely influence visualization by extending the color representation dynamic. Many current outlier filters underperform because they do not account for nonnormally distributed data and codependence of heights on x- and y-axes.

An approach for detecting outliers has been proposed by Le Goïc et al. [101] as follows:

1. Outliers are defined according to close neighbors, based on a multiscale modal decomposition, which has a low sensitivity to outliers in the form of local spikes (Dirac type), a common case. Other multiscale approaches could work, e.g., Fourier, wavelets, or sliding bandpass.
2. Outliers are identified at each scale recursively, using a Grubbs-Base criterion, which identifies and accounts for multiscale groups of outliers.
3. Outliers are excluded before further analysis. Missing height samples can be replaced, taking care that the replacements do not alter the functional multiscale characteristics of data.

This method seeks first to filter out the larger features in the topography that might hide outliers, e.g., upward spikes in valleys, to make the outliers more prominent, and then it applies a statistical test to identify the outliers.

In Brown et al. [38], multiscale curvature analysis was used effectively to detect outliers by identifying regions of exceptionally large curvatures (Fig. 3.7.1). In addition to curvature, which can be approximated by the second finite difference, higher-order differences are also tested. The first spatial derivative is the slope and the second spatial derivative is approximately the curvature [76]. Finite differences are presumed to be preferable to fitting a function approximating the measurements and taking derivatives mathematically, because this faithfully maintains the originality of values in the measurements. In addition to taking finite differences between adjacent height measurements, i.e., at the SI, down sampling is used to look at outlying finite differences at larger scales. It is commonly known that noise in the data is amplified and exacerbated by amplifying irregularities through progressively higher finite differentiations. This exacerbation can be exploited to magnify errors in the data and makes them easier to detect statistically. The multiscale aspect allows for the detection of different sized groups of outliers, as shown in Fig. 3.7.1 [38].

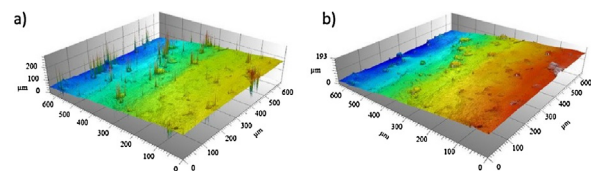


**Fig. 3.7.1.** (a) Surface with outliers as measured by a confocal microscope, (b) surface with outliers removed by application of curvature filter [38].

### 3.8. Scattering

Considering multiscale analysis in the context of this paper, scattering by surface topographies can be divided into two regimes based on the roughness height compared to the wavelength of the incoming signal. Here, we are considering the larger scales for geometric scattering by rough surfaces, i.e., ray tracing off facets, rather than the smaller scales and diffraction. This type of geometric scattering is the basis for many analysis and measurement systems such as BRDF (bidirectional reflectance distribution function), RTI (reflectance transformation imaging), PTM (polynomial texture mapping), and HSH (hemispherical harmonics), which have been reviewed recently by Pitard et al. [126]. These photometric systems are the basis for commercial topographic measurement instrumentation (e.g., GelSight and Cultural Heritage Imaging).

Photometric approaches to understanding scattering reconstruct the topography from the reflected light. Geometric approaches attempt to predict the scattering from the topographic measurements. The apparent scale for the latter systems is the pixel size in the acquisition. There is no apparent scale for the former. Pitard et al. [126] note that the correlations between CPs for rough surfaces and appearance are still problematic.

Shipulski and Brown [149] proposed a multiscale geometric approach. This model for scattering was based on ray tracing and facets on the surface. They proposed a multiscale simulation combined with reflectance measurements to find the scale where the simulation and the measured scattering correspond. The simulation traces rays from a light source that are then reflected by facets on the surface. The percentage of the incident rays from a light source that intersect a sensor at a certain position were calculated. They tested the simulation on a measured surface and demonstrated that the scattering increases with decreasing scale. This ray tracing geometry was illustrated in a paper on gloss and surface topography by Whitehouse et al. in 1994 [190]. The hypothesis, which was not tested, is that the measurement of the actual scattering should match the percentage calculated in the simulation and indicate the scale for approximating the scattering interaction with the topography [149,190]. This simple model

overlooks the finer scale roughness that is certainly within the facet. It also calls for reflectance measurements on highly polished surfaces of the same material to adjust the model for absorption and transmission.

There are a couple of cases of finding good correlation between topography and gloss. Briones et al. in 2006 [30] were able to find a strong correlation on six specially prepared chocolate surfaces ( $R^2 = 0.95$ ), using the MC area-scale complexity in the range of 3–14  $\mu\text{m}$  using a logarithmic regression for the MSA [30]. Vessot et al. in 2015 studied the gloss of 72 different historical photographic papers [183]. The topographies measured with a confocal microscope found strong correlations ( $R^2 > 0.8$ ) when the measurements were made with the 5 $\times$  and 10 $\times$  lenses with an MSA using logarithmic regression. This falls to less than 0.5 with the 20 $\times$  lens and even lower with the 50 $\times$ . The measurements with the 5 $\times$  and 10 $\times$  were marked with numerous spikes that did not appear when using the higher magnification lenses.

### 3.9. Wetting

Multiscale frequently comes up in searches about topography and wetting. Many papers use variations of fractals to construct hydrophobic surfaces, e.g., Bittoun and Marmur [24]. These papers however do not use MAC or MCs in their analyses or characterizations.

Belaud et al. [16] sought to understand the influence of roughness on wettability of isotactic polypropylene treated with femtosecond laser ablation. They combined ISO CPs with the Wenzel and Cassie-Baxter equations. The MAC used Gaussian high and lowpass filters – separately – to do upper and lower open-ended, scale-based decomposition of white light interferometer measurements. Then it calculated the CPs: developed surface area, closed hills and dale areas, and skewness. Correlation coefficients (R) with the contact angle between 0.83 and 0.85 were reported.

### 3.10. Transfer phenomena

Considering Newton's law of cooling or Fick's law of diffusion applied to diffusion through a surface, the total quantity of heat or mass transferred depends on the area of the surface available. It is known from consideration of the fractal nature of irregular surfaces that the area is not unique, but depends on the scale, e.g., of observation, measurement or calculation, which is used to determine it. Therefore, one would expect to be able to find experimental evidence of scale-dependent behavior.

The expected tendencies were found by Karabelchtchikova et al. for carbon in steel [94,95] and by Moreno et al. for oil in fried foods [124]. The former found high correlations ( $R^2 > 0.97$ ) between the MC relative area and carbon flux at 2  $\mu\text{m}^2$ . Hot rolled AISI 8620 steel bars were normalized and machined before preparing several surface topographies by grit blasting, wire brushing, and grinding with abrasive papers. Carburization was done at 925C for 3 h in an endothermic atmosphere, enriched by natural gas with a 0.95% weight carbon potential. There was also a strong correlation with peak to valley roughness. This could be that the peak to valley roughness just happens to correlate well with the relative area at 2  $\mu\text{m}^2$ . In any event, there is no theoretical basis suggesting any probable causation between mass transfer and peak to valley roughness. Similarly, strong correlations ( $R^2 \sim 0.9$ ) were also found for two types of fried foods between surface roughness at specific scales when characterized by the MC relative area and oil uptake [124].

### 3.11. Electrochemistry

Jing and Tang [92] used an AFM (atomic force microscope) to measure variations in thickness of Ga-doped ZnO (GZO) films that were deposited on glass by magnetron reactive sputtering, for 10, 20, and 30 min. A wavelet decomposition was used as the MAC for a six-level decomposition to calculate corresponding MC, RMS roughness, Rq. At the largest scales, the Rq ranked with the

deposition time, whereas at the finest it did not. The box counting FD relates to the grain size.

FDs calculated from AFM measurements and relations to grain size were studied by McRae et al. [118] as well. They used area-scale as the MAC to study anodic oxide grown on a two-phase, Zr-2.5Nb alloy. The smooth-rough crossover derived from the area-scale analysis was comparable to the average width of the minimum grain size. The FD from the AFM also compared well with that calculated from measurements of the electrochemical impedance spectra (EIS), which was based on a fractal model of capacitance.

The discrete wavelet transform (DWT) was applied to SEM images and AFM measurements of nonplatinum group metal catalysts [191]. It is claimed that the work led to a new method to measure scale specific roughness and that the resulting scale specific relationships between structure and properties would support chemical speciation and the performance of fuel cells. Plots of roughness assessed by SEM versus the roughness calculated from the AFM roughness at each DWT level indicated that the SEM roughness cubed is approximately related linearly to the AFM roughness.

### 3.12. Fractography

The fractal properties of fracture surfaces have been known since early publications on fractals [116]. The development of analyses and characterizations resulted in several different FDs in the 1990s, depending on how the calculations were done. In 2000 [113] and again in 2009 [52], strong correlations were found between MCs and work-of-fracture.

In 1996, Bar-On et al. studied the fracture surfaces of hot pressed silicon nitride maximum grain size 3  $\mu\text{m}$  from toughness tests, using a precracked beam [7]. The surfaces were measured with a confocal microscope. Triangular tiling was the MAC that resulted in the MC relative areas [4,83]. Surfaces formed during stable crack growth, compared to unstable growth, had higher relative areas and greater complexities, at larger scales, and larger smooth-rough crossover scales. Because energy is consumed in generating more surface area, they discuss the possibility of an inherent fracture energy for a certain material at a fundamental scale for crack growth.

In 1997, Power and Durham noted that the topographic data for fractures in granitic rocks indicated that fracture surfaces could be characterized as approximately fractal [129]. The surfaces were measured with a contact probe. From 0.1 to 200 mm, the data appeared statistically self-affine according to the MAC, using the slopes of the power spectral density versus spatial frequency.

In 2001, Stach et al. found that the FDs of fracture surfaces in steels change, i.e., are multifractal, with respect to scale [152]. The surfaces of ductile and of brittle fractures in steel were measured with mechanical areal profiling. Two methods were used for the fractal MACs: areal-scale tiling and box-counting, with similar results. At the largest scales, the FDs approach two. The brittle surface had lower FDs, i.e., less complexity, than the ductile. At the finest scales in the study, both surfaces showed a change to greater complexity. The change occurs at a larger scale for the ductile fracture.

In 2000, Malchiodi and Brown used the MAC triangular tiling to calculate the MC relative area [4,83] on graphite electrodes used for melting steel [113]. The graphite was processed under four different conditions. It was fractured by a tapered steel wedge, and the work of fracture was measured. The surfaces were measured with a scanning laser height sensor and characterized over scales from about 0.001 to about 50  $\mu\text{m}^2$ . MSAs were done by linear regression and F-test on the relative areas versus scale. The strongest correlations were found ( $R^2 > 0.91$ ) with the work of fracture at a scale of 3  $\mu\text{m}^2$ . Strong correlations were also found at the finest scales and at about 10  $\mu\text{m}^2$ . Confident discriminations, better than 97.5%, were found, also at about 10  $\mu\text{m}^2$ . Interestingly, the correlations were negative, with greater relative areas and

greater complexities corresponding to lower works to fracture. The opposite tendency was found by Ulcickas in 2000, also using the MAC area-scale analysis to determine the MCs relative areas on yttria-stabilized tetragonal zirconia [175]. They were trying to discriminate surfaces produced during different mechanisms of crack growth. They found that the surface complexities tended to increase as the relative area approaches the average grain size and with increasing fracture toughness.

Cantor and Brown in 2009 studied chocolate surfaces fractured in three point bending at six different temperatures 10–35 °C [52]. The surfaces were measured with a scanning laser height sensor. The MAC was area-scale tiling and the MC was relative area [4,83]. The MSA was done by linear regression. A strong correlation,  $R^2$  of 0.99, was found between relative area and the temperature of the chocolate during fracture at a scale of about 17,000  $\mu\text{m}^2$ . The  $R^2$  values decreased markedly at scales higher, and lower, than this to less than 0.1.

### 3.13. Design

Braatz et al. [29] called for new methods for the design and control of multiscale systems for products that are used in processing that have length scales from nano to macroscopic. The challenge is to integrate physically a number of phenomena that are occurring on different scales simultaneously. In 1994, this problem was addressed in the context of Suh's axiomatic design [164] and MC of rough surfaces [45,31,32,33]. Suh's first axiom states that the independence of the functional elements must be maintained. The third corollary calls for integration of design features on a single physical part, provided the functions could be independently satisfied. Both of these can be accomplished when topographically dependent functions occur at different scales. Multiscale analysis and characterization provide a means of understanding how to maintain functional independence when the physical features fulfilling those functions occur at different scales. Multiscale analysis and characterization supports product and process design when the scales of interaction for surface performance and processing can be separated. Specifically, it was proposed that relative areas as a function of scale could be a useful MC for concurrent engineering design of rough surfaces, essentially achieving physical integration and functional independence through the understanding of scale of interaction. An example is oil lubricated sliding surfaces, as with rotating lip seals riding on a shaft. The shaft should be smooth, to provide a seal, and have a special kind of texture to retain lubricant at the shaft-seal interface. The sealing occurs at a large scale, and the lubricant retention at a fine scale, which should be taken into account in the design of the shaft and the manufacturing processes. Ideally, the same CPs should apply to the verification of functions at the appropriate scales and to controlling the manufacturing process [34].

## 4. Other multiscale applications

### 4.1. Paleontology

Similar to wear marks on tools and workpieces due to manufacturing processes, as described above, the topography of teeth can indicate diet, which is useful in paleontology. Multiscale surface analyses have been especially successful in the characterization and comparison of dental microwear textures, or topographies. The basic idea is that the pattern of wear-related scratches and pits on a tooth's surface can indicate things about diets of fossil species, assuming that hard foods, like nuts or bone, are crushed, causing pitting, whereas tough ones, like leaves or meat, are sheared, causing scratches. Studies of mammalian teeth have borne out these expectations. Leaf-eating primates and meat-eating lions, for example, have more scratches than seed-eating primates or bone-crunching hyenas [182,185].

The traditional method for characterizing microwear surface patterns was limited because it depended on measurement of individual features on SEM images. This suffers from two disadvantages. First, there is information loss when representing a 3D surface in two dimensions. The shadowing effects that give a surface the illusion of depth depend on the angle between electron beam and tooth surface, so researchers scanning a tooth at even slightly different orientations get different indications from the SEM images. Second, observer-to-observer measurement error often runs between about 5–10% [78]. A microwear surface can have hundreds of visible features, the boundaries of which are irregular and commonly overlap the borders of others and the edges of the field of view. It can be difficult to determine the endpoints of scratches and especially pits; in addition, the number of features identified seems to correlate as much to the visual acuity and persistence of the researcher as anything else. Taken together, these issues can introduce noise to the diet signal and limit the potential of microwear to reveal food choice.

Dental topographic analysis was introduced as an alternative method for quantitative characterization of microwear patterning. The new approach involved automated whole-surface characterizations, using white-light scanning confocal profilometry combined with scale-sensitive fractal analysis [179,141,142]. A multiscale approach was chosen because teeth function at multiple scales and because tooth structure, and, hence, its responses to chewing loads, is multiscale [177,178].

First, teeth function in breaking down food at a variety of scales – they act as a guide for chewing motions at a gross scale, and as tools for accomplishing food fracture at finer ones (consider a steak knife, with a sharp blade split by serrations). Moreover, abrasives that wear a tooth surface represent a variety of scales – there are sharp, angular edges to natural silica, whether adherent grit or endogenous silicates, within plants. There is also the diameter of the abrasive itself and the diameter of the food particle, which reduces with each chew.

Tooth responses to loads and abrasives are also expected to vary with scale because of enamel micro and nanostructure. Tooth enamel wear surfaces are roughly fractal in nature (Fig. 4.11). Hydroxyapatite nanospheres form at a diameter of about 20 nm, and agglomerate to 60 nm units. These, in turn, combine into nanofibers that bundle together by the thousands, like spaghetti bunches, to form single rods, or prisms, each about five microns in diameter. And these prisms, in turn, are bundled together by the thousands to form an enamel surface [59,81,205].

The MCs area-scale fractal complexity [4,83] and length-scale anisotropy of relief have been especially effective tools for measuring molar microwear topography. They have been shown to be capable of distinguishing mammals by diet, from ruminants [120,121,139,179] to carnivores [69,137,180], rodents [49,53], marsupials [130], and even armadillos and sloths [80]. Microwear surfaces with highly complex textures, such as those with pits of many sizes, are typical of species that consume hard objects, whereas anisotropic textures, those dominated by aligned striations, are typical of species that eat tough foods [66].

These scale-sensitive approaches contrast with another approach, which is not expressly multiscale but gaining popularity for characterizing dental microwear topography. It involves using many of the texture characterization parameters defined by the International Organization for Standardization (ISO/CDIS 25178-2 [83]). Commonly used ISO parameters include measures of feature depth (e.g., Sv, S5v), area (e.g., Sda), volume (e.g., Vvv, Sdv), anisotropy (e.g., Str), complexity or developed surface area (e.g., Sdr), density (e.g., Ssk), and a bevy of others [83,165]. These, too, have been used to characterize microwear textures for a broad range of mammalian taxa, from primates [51,65] to ruminants [138], bats [131], elephants [203] and pigs [150], to name a few. These ISO standard characterization parameters have been employed because of their wide availability. The basic idea seems to be to apply every standard measure available in a software package and see which parameters separate groups. There may

even be more variables considered than there are specimens to be contrasted. A few of these parameters exhibit useful scale sensitivity, such as developed area (Sdr), which has been shown by Burglund et al. [18] to correlate with the relative area at fine scales in a paper comparing functional correlations using area-scale analysis and ISO parameters.

Scale-sensitive approaches that begin with an appreciation for the processes responsible for wearing teeth can be preferable conceptually. Tooth wear is brutally complex and occurs at many scales (whether considering the wear surface, the food surface, or the process of wear). To characterize tooth wear appropriately, a scale-sensitive approach offers a stronger logical foundation.

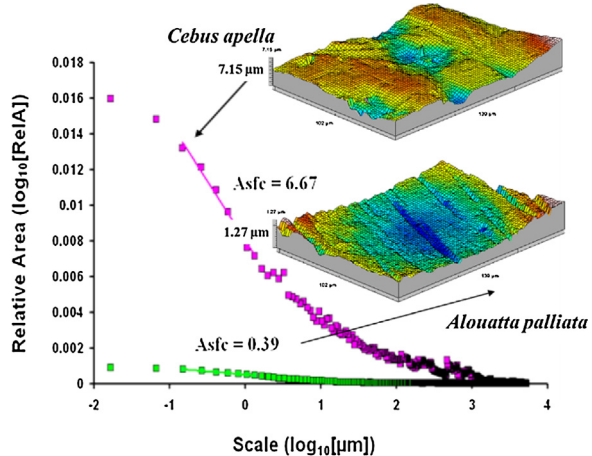


**Fig. 4.1.1.** Area-scale comparison of micro dental wear hard-object feeding monkey (capuchin) above and a tough leaf-eating one (howler) below.

#### 4.2. Archaeology

Multiscale topographic analysis on stone tools is an outgrowth of traditional microscopic use-wear or microwear analysis that first developed in the early to mid-twentieth century in order to identify used portions of tools, the motions of the tools, and the types and hardness of materials contacted. Identification of use-wear on prehistoric artifacts is based on comparisons to tools used in experimental archaeology and ethnoarchaeology [163]. Criticisms that optical microscopy was too subjective and analyst-dependent and that it lacked reliability [71] led archaeologists to attempt other means to study surface wear — specifically focused on the characterization of measured surface topographies [163].

The first MAC of experimental stone tool surface roughness was performed by Stemp and Stemp [161,153], based on plots of  $\log R_q$  versus  $\log$  evaluation length ( $R_q\text{-el}$ ). Profiles were measured with a laser profilometer on the surfaces of both used and unused chert and obsidian flakes, demonstrating that laser profilometry was effective at documenting stone tool surfaces, and that  $R_q$  changed with evaluation length. In another experiment, now using MSA as well as MAC, chalk flint flakes used to saw pottery and wood could be discriminated from the same surfaces before use, using laser profilometry and  $R_q\text{-el}$  [162,153]. Wear determined by increasing numbers of strokes could be discriminated, based on  $R_q\text{-el}$  for the pottery-sawing flakes. A failure to discriminate surface topographies with increasing use on the wood-sawing flint flakes was attributed to poor measurement location selection.

Following the encouraging results of these experiments, additional experiments were undertaken with chalk flint flakes used on shell, wood, dry hide, and soaked antler [156,153]. The surface roughness profiles in the unused and used regions were documented using a laser profilometer and discriminated using the relative length MC [4]. As in the previous experiments, the use-wear on the tools varied with scale. When the relative lengths for

the tools used on different contact materials were compared, MSA results indicated that discrimination of surface roughness due to wear was statistically significant at different scales [156,153]. A second test of the ability of laser profilometry and RL to discriminate surface roughness in unused and used regions of chalk flint flakes [155,153] produced similar results to the first with discrimination occurring at different length-scales, depending on which tool regions were compared.

Relative areas (Srel, MCs) from area-scale analyses [83,4], MACs, have discriminated unused and used regions of hide-cutting and wood-sawing obsidian flakes [157]. The discrimination (F-test versus scale, MSA) was noted to be more confident at the finest scales in the confocal microscopic measurements. Stemp et al. [154] found that obsidian blades used to replicate ancient Maya blood-letting (with 30 strokes in raw beef) could be discriminated with MSA (F-test versus scale) from the unworn surface with the MC Srel [83,4] at coarse scales; and the fine scales, where use-wear should be detected, only on one blade. The original structure of the obsidian surfaces (smooth versus microstepped), the direction of tool use, and the condition of the contact material were all thought to be important variables affecting use-wear development and the discrimination of surface roughness.

Stemp et al. [158], using two different types of quartzite scrapers, discriminated surfaces used on both fresh and dry deer hide with the same measurement and analysis methods of MSA of MCs. In all instances, surface topographies could be discriminated to varying degrees at different scales. Fresh hide scrapers were discriminated from the dry hide scrapers at fine areal scales, whereas the unused surfaces of the scrapers made from different types of quartzite were successfully discriminated at medium scales, consistent with variation in the structural properties of the stone types themselves. The same scrapers were tested using the MC area-scale fractal complexity (Asfc) [4,83,159], and certain discriminations were more confident at finer scales.

Key et al. [97] used basalt flakes to cut oak branches with loads ranging from 150 g to 4.5 kg, also using scanning laser confocal microscopy (SLCM) and relative areas. Of the 23 flakes, many were discriminated at fine scales. Above about 750 g working load differences, the use-wear could be discriminated at fine scales. Below about 750 g, load differences between 250–750 g were necessary for discrimination. Using Asfc as the MC on the same measurements extended discrimination of loading conditions to fine scales. The MSA F-test could discriminate the worn surfaces of most of the 23 basalt flakes, when the difference in load was above about 100 g. Asfc appears to be better, as an MC, for discriminating loading of worn basalt flakes at fine scales than relative area [160], which is logical because Asfc is essentially the scale-based derivative of the Srel, and therefore is not influenced at the fine scales by large scale changes, as is the Srel. In Fig. 4.2.1 the results of an MSA are shown as the mean square ratios (MSR) from an F-test of area-scale fractal complexity (Asfc) for basalt flakes with a 2532 g versus a 1767 g load. Strong discrimination of the two flake surfaces is above the 95% confidence level, as represented by the solid horizontal line marking between about 0.25 and 200  $\mu\text{m}^2$ .

Álvarez et al. [3,72] discriminated use-wear on experimental stone flakes made from rhyolite using variograms and MC which based on the characterization of roughness using the log-log of variance ( $\sigma^2$ ) versus area sizes ('observation windows') on the digitized images to determine FDs as a function of scale from the slope of the curve. The intersections of the different plotted slopes provide the crossover lengths necessary for surface characterization. The experimental flakes used to scrape bone, hide, and wood were discriminated using this method.

Lesnik [106] studied worn surfaces of bone tool artifacts excavated from Swartkrans, South Africa (1.8–1.0 million years old), to determine their potential use as implements to dig into termite mounds as a food source for early hominids. On a series of epoxy resin casts of experimental bone tools and bone artifacts, worn surfaces were measured, using an LSCM and MCs Asfc [83,4], scale of maximum complexity, anisotropy, heterogeneity, and

texture fill volume. The only parameter that demonstrated significant statistical differences on surface topography using ANOVA was Asfc.

To better understand craft-production using bone tools by the Ancestral Pueblo society (850–1140 CE) from Chaco Canyon, New Mexico, Watson and Gleason [187] studied experimental tools that replicated the processing of perishable materials (e.g., deer hide, yucca, birch bark, sandstone, ceramic), measured with a scanning laser confocal microscope. With the MCs Srel and Asfc, confident discrimination of plant-working and hide-working bone tools was found at larger scales, discrimination of sandstone-abraded and plant fiber-abraded bone tools at larger scales; and a sandstone-abraded tool was significantly discriminated from a hide-scraping tool only at fine scales. These results demonstrate the potential application of scale sensitive fractal analysis to bone artifacts to determine tool function and comment on past economic activities.

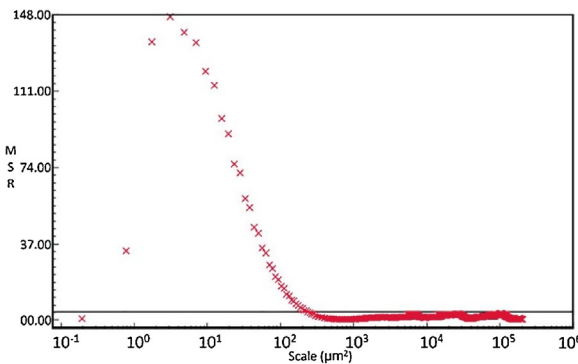


**Fig. 4.2.1.** The MSR (mean square ratio) from an MSA f-test using the MC complexity for discriminating loads on worn basalt flakes [160].

### 4.3. Geography

In the geographic sciences, MAC is often achieved by varying the resolution, i.e., SI, of the Digital Elevation Maps (DEMs). The SI is indicated as a prefix to the data, e.g., 5 m data, and is varied during acquisition and by resampling, or down sampling. Elevation data is fundamental for environmental sciences and water resources management for watershed-level analysis, modeling of water quality and quantity, sediment load, peak flow, soil erosion, and landslide risks. New measurement technologies, such as, LiDAR (Light Detection and Ranging), provide better detail and resolution for geography. Then, there is the question of which scales should be used for modeling.

Gao [75] showed how accuracy, through the calculated mean gradient, i.e., slope, an MC in this application, decreases with increasing SI (Fig. 4.3.1). The slope at a location is determined by a finite difference of the elevations of the 8 surrounding tiles and the sampling interval to determine the average slopes in the x and y directions, averaging the two slopes from three elevations, and then taking the square root of the sum of the squares [68].

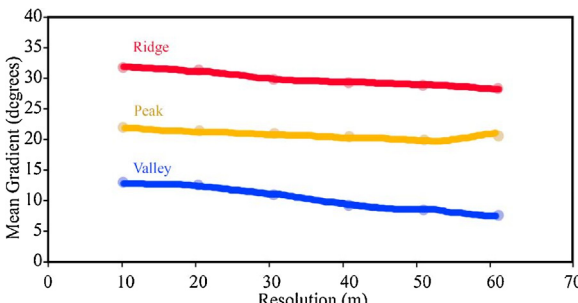


**Fig. 4.3.1.** Influence of resolution on terrain gradient, or slope, at six resolutions or SIs [75].

Usery et al. [181] demonstrated that with a decrease in resolution of DEMs, a general degradation of both elevation and land cover correlations is noted which has implications on watershed-level modeling. Few recent studies have shown that finer-resolution DEMs (e.g., LiDAR-based DEMs at 5 ft. or 1 m resolution) might not necessarily model environmental processes in the same manner and produce similar results to their coarser-grained counterparts, e.g., 10 m RADAR/Topo or 90 m SRTM data [79,67]. Further, studies have shown that DEMs obtained at 90 m original resolution and 30 m resample to 90 m do not produce the same results. Meirose et al. [119] showed that stream delineations are significantly different at different resolutions and resampling. They used area-scale analyses to show decreased relative areas and area-scale FDs (Das [83]) with resampling, which makes Das an MC in this particular application. There are corresponding differences in the watershed modeling (Fig. 4.3.2).

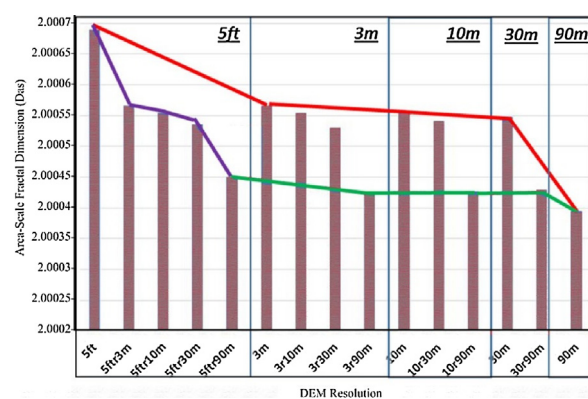


**Fig. 4.3.2.** Area-scale FD from Quadrangle #1 on all Center Ridge Watershed, FL, USA, DEMs for 5 ft, 3 m, 10 m, 30 m and 90 m with resampling as indicated, e.g., 3x10 m. Red and green lines show changes with measured SI and resamplings to 90 m respectively. Purple shows down sampling of 5 ft data [119].

## 5. A synopsis of methods

The previous two sections have dealt with applications of multiscale analyses. The objective of this section is to provide a synopsis of multiscale methods to serve as a foundation for the syntheses in Section 6. This section begins with scale decompositions based on spatial frequencies and continues with multiscale geometric approaches.

### 5.1. Conventional multiscale methods

A **closing or an opening morphological filter**, using defined structuring elements, creates morphological envelopes. The closing filter creates the upper envelope of the surface, which contains most of the protruding peaks and structures but removes a few of the deepest valleys and lowest structures. For example, the closing profile obtained with a disk-structuring element of 2 micrometers of radius corresponds to the ‘traced profile’ measured by a stylus profilometer. A closing filter is composed of two subsequent morphological operations, a dilation followed by an erosion. Symmetrically, an erosion followed by a dilation obtains the lower envelope, created by an opening filter. Multiscale morphological filters are defined in ISO 16610-49 for profiles and ISO 16610-89 for surfaces, and are named scale-space techniques.

As the envelope does not exactly follow the surface (Fig. 5.1.1), there are voids in between the surface and the envelope, and the larger the structuring elements, the bigger the void volume. When a series of envelopes is generated with increasing structuring element sizes – considered as scales of analysis, it is possible to calculate the void volume at each scale and draw a log graph of the void volume as a function of the scale. Several parameters can be

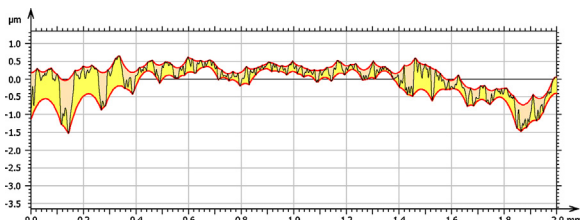


**Fig. 5.1.1.** Grinding profile with its upper and lower envelopes, generated by a disk of 5 mm radius.

calculated globally or at a given scale. This method is described in ISO 25178-2 [83], as the Svs curve (volume-scale). It is similar to other classical fractal methods such as the box method or the tiling methods (see Section 5.5).

**Fourier transformation** converts spatial information to spectral information, which make it possible to assess the frequency content of the profile or surface. As frequencies, or wavelengths, can be seen as lateral scales, the frequency spectrum, or the power spectrum (square of the Fourier amplitude), provides an evaluation of the magnitude of each scale from the shortest (Nyquist limit =  $2 \times$  lateral spacing) to the largest (lateral dimension of the data).

This method is commonly used in optics to evaluate roughness and waviness (mid-spatial frequencies) on relatively smooth geometric forms. The **Power Spectral Density** (PSD) is calculated on lines, columns, or various directions of a surface and displayed on a log-log graph (Fig. 5.1.2). ISO 10110-8 [210] describes a limit line for specification and verification to control the quality of fabrication.

Multiscale analysis may be carried out by **multiple measurements**, for example, with different magnifications on a microscope (using different objectives) or with different measurement techniques on the same sample. Usually, when reducing the scale of measurement (increasing the resolution), the dimension of the measured area is reduced. It can be compared with a series of pictures taken with a zoom at different settings. The closest zoomed image has more detail, but it only contains a small portion of the complete picture.

When using several instrument types, it is necessary to resynchronize the two (or multiple) images with a fitting, taking into account the lateral shift, the difference in resolution, the rotation of the field of view, and occasionally its geometric deformation. For example, resynchronizing can be required with a scanning electron microscope (SEM) used to zoom in on a particular feature and a confocal microscope used to get the complete sample image. Besides the multiscale aspect of the analysis, it is also frequently a means to get complementary information provided by the different measurement principles. For example in the case of an AFM measurement relocated on a fluorescence microscope, it is possible to superimpose the topography with the active parts of cells (fluorescence) and the friction of the cell membranes (given by the AFM). These techniques, which are applied to the combination of measurements made at different resolutions by different instruments, are sometimes referred to as *data fusion*, *colocalisation*, or *correlative metrology*.

## 5.2. Wavelets

The early studies of morphology features of surface topography only considered the roughness component of surface texture. Comprehensive studies of surface characterization have nearly always concentrated on roughness assessment and mainly developed evaluation techniques based on parameters and filtration techniques covering a broad range of scales.

Wavelets record the true nature of the real waveform, shape, and amplitude within a permitted cut-off wavelength or scale. During the last two decades, novel filtering techniques, based on wavelet techniques, have been developed [206,196]. Wavelet filtering is designed as a MAC for the analysis of multiscale

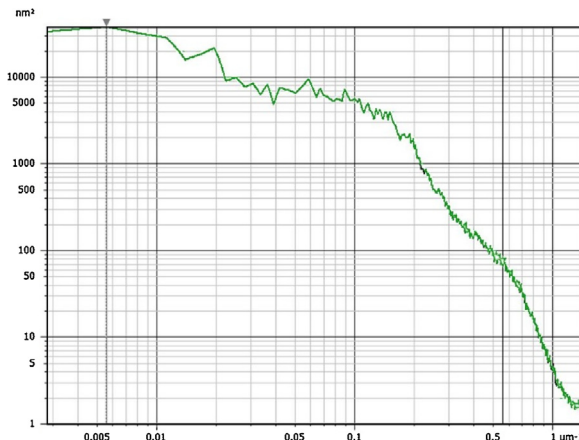


**Fig. 5.1.2.** PSD (Amplitude versus spatial frequency) calculated on a wafer-back after several passes of grinding and before polishing.

functional surfaces, including nanoscale surfaces. The benefits of using wavelet filtering are the extent of the filtered surface range and that there is much less distortion of the filtered surface within this cut-off wavelength than has occurred from conventional methods. Consequently, wavelet filtering is guaranteed to obtain a scale-specific roughness surface, e.g., nanoscale, with a high level of fidelity within this cut-off wavelength for MC.

Biorthogonal wavelet filtering for surface analysis was proposed by Jiang et al. [85]. It has been carried out to extract directly the different components of the surface topographies for MC. The first generation wavelet transform was applied for the comprehensive identification and evaluation of multiscale functional features of these surface topographies. In this work, measurement of the femoral heads and acetabular cups was carried out to demonstrate the applicability of the characterization technique for the three-dimensional surface topography of orthopedic joint prostheses.

Second-generation wavelet representations, using a lifting scheme, were developed and successfully applied to surface measurement denoising and to separate and reconstruct different surface components with a fast algorithm [86,87]. The second-generation wavelet transform algorithm is much easier and faster than conventional filtering methods, and the transform procedure only embraces three stages: 'plus', 'minus', and 'application of the weighting algorithm.' All computations are carried out in-place through rows and columns; no extended memory is needed. The process extracts surface features such as peaks and pits unambiguously.

A complex wavelet model (the third generation wavelet transform) was introduced by Jiang et al. [85] to solve the problems of nanometer roughness analysis of surface texture, in which small shifts of the input signal can cause large variations in the distribution of energy between wavelet coefficients at different scales [88]. By the proposed method, shift-invariant separation of multiscale features can be achieved. Zeng et al. [199] have proved that metrological characteristics of complex wavelet transform for surface analysis can be improved, especially for transmission characteristics. The property of zero/linear phase by the dual tree complex wavelet transform (DTCWT) ensures filtering results with no distortion and adequate ability for feature localization. Due to the 'steep transmission curve' property of the amplitude transmission characteristic, the DTCWT can separate different frequency components efficiently for MC. A complex finite ridgelet transform (CFRIT), which provides approximate shift invariance and analysis of line singularities, has been proposed, taking the DTCWT on the projections of the finite Radon transform (FRAT). The numerical experiments show the remarkable potential of the methodology to analyze engineering and bioengineering surfaces with linear scratches in comparison to wavelet-based methods developed in previous work [90].

As pointed out by Jiang et al. [89], engineering surfaces have undergone a significant development, and more and more complicated freeform surfaces are being produced. These new surfaces have more complicated geometries with nonEuclidean nature. The nonEuclidean surfaces require new wavelet tools that can analyze such surfaces. A generalized lifting scheme to filter the texture of freeform surfaces represented by 3D irregular triangular meshes was proposed [1]. A new multiscale triangular mesh, based on freeform surface texture filtration, using a Laplacian mesh relaxation scheme, has been presented [84]. It needs to be pointed out that both of these methods require a form-removal stage before they can be applied.

Contrary to the usual use, mainly based on multiscale filtering of surfaces, the approach developed by Zahouani and co-workers from 1998 to the present [5,105,122,134,151,194,195,196,197,198], focuses on the use of continuous wavelets. These transform, locate, and quantify the amplitudes of the topographic signal, from roughness to the waviness in a wide band of wavelengths, without any break in the wavelengths.

Not only does this approach represent a multi-wavelength analysis tool, it is also a multiscale quantitative method. For example, it is possible to characterize a topographic component by calculating a topography parameter for each scale 'a'. The SMA or roughness spectrum is the calculation of the topography coefficient  $Sa$  (arithmetic mean) at each resolution level (scale) of the signal, where  $|W_a(x,y)|$  are the absolute values of the amplitudes of the multiscale decomposition.

$$SM_a = \sum_{x=1}^{Ny=M} \sum_{y=1}^{M} |W_a(x,y)| / MN \quad (5.2.1)$$

A second important advantage of this multiscale quantitative method is that it makes it possible to compare two surfaces in all the wavelength ranges in a quantitative way, without worrying about repositioning the topographic images as in the case of inter-correlation of two images. This multiscale comparison approach demonstrates all its effectiveness for the problems of wear in tribology, archeology, bioengineering and manufacturing processes. The example of Fig. 5.2.1, illustrates the potential of the method in wear. In this case, it is the study of the wear on the roadway topography by a simulator of wear on the pneumatic pavement contact. This example shows the relevance of multiscale analysis in the different stages of wear with the multiscale comparison of the topography components as a function of the number of friction cycles, which suggests the results in Fig. 5.2.1.

### 5.3. Sliding bandpass filtering

One method for achieving MC of surface topography is to apply a series of bandpass filters, with varying center wavelengths and bandwidths, on a data set (MAC), as demonstrated in Berglund et al. [17,101], and more recently in Blateyron [25], with the purpose of creating scale-limited datasets. The bandpass filters can be constructed from combining conventional lowpass and high-pass filters. The scale-limited datasets can then be characterized using any CP, e.g., for correlation or discrimination.

$$MCF(\%) = \frac{SMa(a)[Worn Surface] - SMa[Initial Surface]}{SMa[Initial Surface]} \quad (5.2.2)$$

Berglund et al. [17], showed with MSA that strong correlations,  $R^2 > 0.9$ , could be found between six conventional CPs and friction in sheet metal forming when analyzed at the appropriate scales. In contrast, with conventional filtering, only two CPs showed stronger correlation than  $R^2 > 0.7$  (non MSA). In that study, the MSA was achieved by bandpass filtering with combined Gaussian high- and lowpass filters. Three different bandwidths were used: 20, 50, and 100  $\mu\text{m}$ . The bandpass filters were used with a range of center wavelengths from 10 to 180  $\mu\text{m}$ , shifted in increments of 10  $\mu\text{m}$ . Conventional CPs were then calculated for all filtered datasets. The MCs were then regressed with the functional

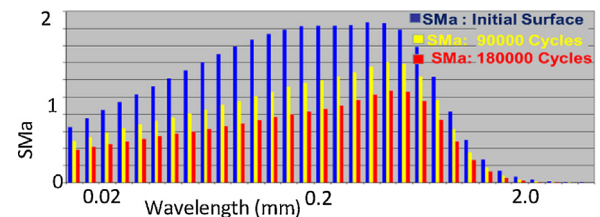


**Fig. 5.2.1.** Quantification of the multiscale amplitude parameter (initial topography (blue color), topography after 90,000 cycles (yellow color), topography after 180,000 cycles).

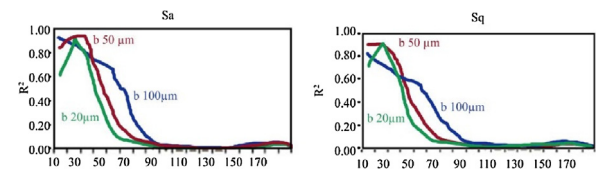


**Fig. 5.3.1.** Correlation coefficients,  $R^2$ , for Sa and Sq, two of the CPs with the strongest correlations to friction. Results from filters with three bandwidths (b) are shown with their center wavelengths [17].

parameter coefficient of friction from bending under tension testing, Fig. 5.3.1.

### 5.4. Structure function

The structure function is related to the autocorrelation function but is without some of its disadvantages, and it has been proposed as a means of quantifying variations in surface texture [136]. Both profile and surface structure functions can be computed, and the latter shows the effect of anisotropy on roughness. The structure function is inherently multiscale, since it is calculated for all available wavelengths in a data set.

The surface structure function  $S(r, \theta)$ :

$$S(r, \theta) = E\{[z(x, y) - z(x, y + r(\theta))]^2\} \quad (5.4.1)$$

where  $z(x, y)$  is the surface height at coordinates  $(x, y)$  in the plane of the surface and  $z(x, y + r(\theta))$  is the surface height at a radial distance  $r$  from  $(x, y)$  in direction  $\theta$  [136].

Many machined surfaces are more or less anisotropic; their finish has a pronounced lay or directional character. The statistical properties of a profile through such a surface will depend on its orientation with respect to the lay.

Fig. 5.4.1 shows an isometric projection of half of a complete three-dimensional structure function of a ground surface. The  $\tau_y$  axis represents the direction of the lay. The variation of roughness with direction can be seen: for instance, the values of the structure function parallel and perpendicular to the lay at a spatial distance of 600  $\mu\text{m}$ . Here,  $S(0, 600) = 6 \mu\text{m}^2$ , while  $S(600, 0) = 12 \mu\text{m}^2$  [136].

In Rosén et al. [133], the structure function was used for finding an appropriate scale for analysis and for relating processing steps to resulting topography at different scales. This study is described previously in Section 3.5.

In Thomas and Rosén [168], the structure function was used for finding the optimum SI in roughness measurements for rough contact mechanics. A method for choosing SIs was proposed, based on Archard's observation that repetitive contact must be elastic. From a description of the rough surface as a self-affine fractal, the second moment of the power spectrum can be expressed in terms of fractal parameters, which are intrinsic properties of the surface. The moment integral is then solved for its lower limit, which defines the tribologically appropriate SI. Thus, a relationship can be derived between three dimensionless numbers: the ratio of this critical wavelength to the topography, the FD, and the material property ratio. Measurements on two commercial hard disk drives were interpreted in terms of the model, and it was predicted that, under realistic operating loads, the real separation between slider

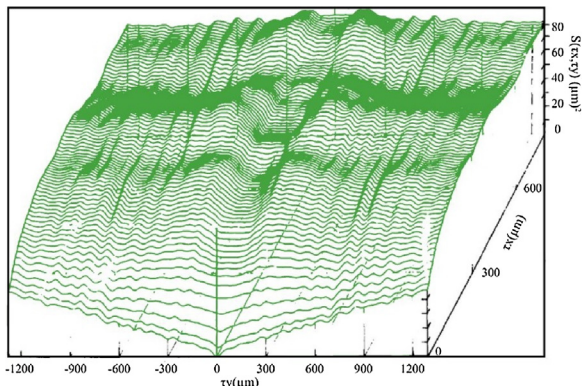


**Fig. 20.** [(Fig. 5.4.1)] Structural variation over a rough ground surface. A quadrant of the three-dimensional structure function of a ground surface reflected about the  $ty = 0$  axis. The lay direction is parallel to the  $ty$  axis [136].

and disk at rest is about 100 nm, with between 40,000 and 80,000 discrete contacts of 12–15 nm radius.

For optics, a two-quadrant area, structure function analysis has been developed by He et al. [207,208]. It was shown to be able to characterize surface anisotropy for all wavelengths available in the measured data. Hvosc and Burge as well as Parks showed how the structure function could be used to specify and analyze form errors of a telescope mirror [209,211].

### 5.5. Geometric

Geometric properties of rough surfaces can change with the scale of observation, i.e., measurement or calculation. The question about the length of the coastline of Britain, a classic example, was posed by Richardson [115] and later used in developing statistical fractals by Mandelbrot [116]. This work showed that the log of the apparent length of irregular lines could vary linearly with the log of the scale of observation in such a way that the coast of Britain can be distinguished from other coastlines, like South Africa, by the slope of the plot. This observation contributes to the development of fractional, or fractal, dimensions to characterize the geometric nature of irregular, or squiggly, lines [116].

Geometric approaches to multiscale analyses are summarized in Table 5.5.1. Derivatives here are finite differences. The digital nature of measured surfaces was recognized and was not smoothed to fit a continuous function to the measured heights. Rather the surfaces can be considered continuous although not necessarily differentiable, like fractals [116].

#### 5.5.1. Length-scale

**Table 5.5.1**  
multiscale geometric analysis.

Theme	Geometric feature	MC	Scale derivative
Dimensionality			
1d	Length	Relative length	L-s complexity
2d	Area	Relative area	A-s complexity
3d	Volume (Filling)	Texture depth	Not used yet
Spatial derivatives			
1st	Slope	Not used yet <sup>a</sup>	Not used yet
2nd	Profile curvature	Linear statistics	Not used yet
2nd	Areal curvature	Tensor statistics	Not used yet

<sup>a</sup> Not yet in the production engineering literature. Slope is used optics, but not in the multiscale sense defined here. Slope scale analyses and characterizations are in the geology literature [201].

Length-scale analyses was used by Underwood and Banerjee [176] on fracture surfaces. They noticed a reversed sigmoidal curve when the coastline method was applied to fracture surfaces.

The coastline, Richardson, compass and length-scale methods all have the same basic approach. The length of a profile is

measured as a function of scale by repeatedly stepping along with a compass or dividers. Alternatively, it could be repeatedly tiled with line segments. The separation on the dividers or the length of the tile represents the scale. On each repetition, the scale changes often from the SI to the length of the profile.

The result compares scales with the apparent profile lengths, determined by multiplying the separation of the dividers (scale) by the number of steps. Only full steps are counted. Often this is presented on a log-log plot of apparent lengths versus scales (length-scale plot, Fig. 3.1.3).

In the standard ASME B46.1 [4], the apparent lengths are divided by the nominal, or straight-line, length of the tiled portion of the profile, to determine a relative length, Rel, an MC. The relative lengths tend towards one, the minimum value, at the largest scales, if the profile is level and the measured profile is long enough. At the large scales, where the relative lengths are close to one, the surface would be essentially smooth. At a sufficiently small scale, called the smooth-rough crossover (SRC), the relative lengths are sufficiently above one, so that the surface can be considered rough below this scale.

The relative length is related to the inclinations or slopes on the surface:

$$Rel(s) = \sum_{i=0}^n \frac{1}{\cos\theta_i} \frac{l_i}{L(s)} \quad (5.5.1.1)$$

In Eq. (5.5.1.1), the total length of the tiled profile is  $L$ ,  $\theta_i$  is the inclination of the  $i^{\text{th}}$  step, and  $l_i$  is the length of the  $i^{\text{th}}$  step projected onto the datum. The second term in the summation is the weighting factor. Note that, if the profile is not leveled, then the relative length at the largest scales is the reciprocal of the cosine of the angle between a level datum and the actual.

One way of calculating an FD is one minus the slope of the length-scale plot [116]. The FD for manufactured parts tends to vary with scale more than natural surfaces, like fracture [6] or clouds [110]. Therefore, the complexity, which is negative a thousand times the slope of the length-scale plot (ASME B46.1 [4]), is another MC. Complexity can have higher regression coefficients for correlation and percent confidence because it indicates the change with respect to the local scale and therefore is uninfluenced by larger scale features, as the relative length is.

#### 5.5.2. Area-scale

The extension from length of profiles to the areas of irregular surfaces is straightforward. A measured surface ( $z = z(x,y)$ ) is tiled with triangles [36,41], like tiling a profile with line segments. The MC relative-area is plotted versus scale (log-log), and a FD is two. The slope of this plot and the complexity is negative one thousand times the slope [4,83]. Inclinations on the surface are related to the relative-area as shown in Eq. (5.5.1.1).

Area-scale has clear physical interpretations and is a logical extension of a discrete interaction theory. This theory proposes that interactions with a surface, such as adhesion [46], require a certain amount of space on the surface and therefore more available area in the topography will provide more possibilities for interactions and stronger reactions per nominal area. Equations for heat and mass transfer, as discussed above, include area, without indicating the scale at which the area should be considered.

Area-scale analysis has the potential to contribute to work on finding fundamental scales of interactions for many kinds of topographically related phenomena. The relative area could serve as a first approximation. It could be modified to consider certain kinds of features, like narrow valleys, and phenomena, like the lotus effect, that might limit or modify interactions [70].

#### 5.5.3. Filling-scale

Filling-scale calculates the space as a function of scale available between a profile or surface topography and a reference line or plane. It has been used to find correlations with the topography of dressed grinding wheels as a function of dressing conditions [39]. It

has the potential to indicate the chip- and lubricant-carrying capacity of grinding wheels and to identify scales in wear phenomena. It is similar to the bearing area in assessing the material versus void in a topography, although it also indicates how this changes with scale. Filling-scale can discriminate a surface and its inverse, which the simple length and area analyses cannot. Although there are more elaborate, length and areal tiling methods that can detect these differences [43,35].

It might seem that a volume analysis, like this, could be the next logical step in the length and area sequence. An FD has not been associated with filling-scale, as with length and area, and is impossible, because there is no fourth physical dimension into which a volume can extend, as profiles and areal measurements extend into the second and third dimensions.

#### 5.5.4. Slope-scale

Slope varies in magnitude and direction with scale and with position. It has been largely underutilized in multiscale analyses and characterizations. It is used by geographers who note that slope changes with scale (section 4.3). Relative length as described by Eq. (5.5.1.1) relates to the inclinations, or slopes, of the tilings. Potentially, for each scale, statistical distributions of those slopes can be created and statistical measures can be calculated. Bartkowiak and Etievant (in progress) studied 3D orientations of normals to triangles. The scale is the size of the triangles, changed by multiples of the SI. They computed the multivariate dispersion statistical parameters for slopes, calculated from directional cosines of triangles' normal vectors. The orientation angles can also be estimated from measurement data for each scale, using the covariance matrix method [11,12]. This MSA has been performed over a set of topographies of twenty different photographic papers [183]. Strong correlations, using nonlinear regression, were observed between gloss reflectance and certain MCs, suggesting potential for slope.

There exist other works related to multiscale slope analysis but related to larger scales. Young et al. [193] introduced an MC, called vector dispersion, to study the accuracy of underwater topographic measurement in multiple scales.

#### 5.5.5. Curvature-scale

Curvature, like area, naturally varies with scale. Because curvature is approximately the spatial derivative of the slope, it requires no datum, whereas heights or slopes do require a datum. This can be valuable when the datum is not obvious, such as in characterizing tomographic measurements. In addition, curvature can indicate convex and concave regions. The former are important in contact mechanics, and the latter can be significant in fatigue and in fracture mechanics. Curvature analysis can identify microgrooves and holes, which act as stress concentrators. It can be also helpful in identifying lay, or surface directionality, i.e., anisotropy, by analyzing the orientation of maximal and minimal curvature vectors. Finally, because curvature is a tensor, it is possible to calculate gradient, divergence, and curl, which can help in improved characterization of particular surfaces.

MAC for curvature determines higher linear or spatial derivatives in order to estimate, locally, principal or directional curvatures. This enables studies of their values and distributions.

Multiscale curvature analysis of profiles (heights  $z$  as a function of position  $x$ ,  $z = z(x)$ ) has recently been developed and has proven useful in providing strong correlations ( $R^2 > 0.96$ ) with the fatigue limit [184]. In that example, curvature is calculated by Heron's formula, which is based on three heights equally separated laterally [76]. The lateral spacing of the two exterior heights is used to represent the scale. For the MAC of curvature from three measured heights, the algorithm steps along a profile, calculating the curvature as a function of position at one scale, and then the calculation repeats for each scale. The other approach is to apply a discrete formula for curvature of a graph in form  $z=z(x)$  as shown by Brown et al. [47]. In that method, the curvature and other spatial finite differences were used to remove outliers from measured topographies.

For MAC for curvature tensors from areal measurements Bartkowiak et al. [13] developed a method based on Theisel et al. [167], where the surface normals are calculated first from measured heights. Down sampling is used to adjust the scale. The regular array in  $x$  and  $y$  of measured heights ( $z$ ), is tiled to create right-angled, and isosceles triangular patches in their ( $x,y$ ) projection. The scale of the calculation is the length of the equal sides. The distributions of maximal, minimal, mean, and Gaussian curvature can be regressed with processing and functional parameters. The method has been used successfully to describe new types of surface textures that are created by conventional machining [10] and additive manufacturing [13]. It can also be used to visualize and characterize surface features that are evident at particular scale or range of scales (Fig. 5.5.5.1).

Alternatively, the Directional Blanket Covering (DBC) [127] calculates curvatures using the first and second derivations of a quadratic polynomial, approximating a local surface profile at a particular scale and direction. The curvature, peak, and valley dimensions are calculated as the slopes of lines fitted to data point subsets of log-log plots of surface areas. Differences between dilated and eroded surface curvature matrices are plotted against scales of calculation. The dimensions quantify directional changes in the overall curvature and the curvature of peaks and valleys at individual scales. The scale corresponds to the center of the subset.

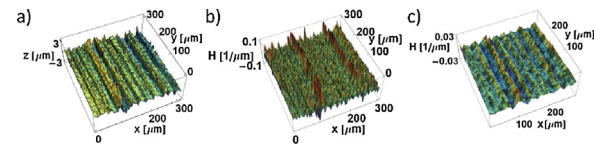


**Fig. 5.5.5.1.** (a) Ground surface measured with confocal microscope, (b) mean curvature ( $H$ ) calculated at scale equal to  $3.125 \mu\text{m}$ , and (c) mean curvature ( $H$ ) calculated at scale equal to  $9.375 \mu\text{m}$ .

#### 5.6. Segmentation

Segmentation is the partitioning of a topography dataset into regions, according to certain properties [140]. Segmentation may be used to identify and isolate a topographic formation from its surroundings, to decompose a topography into its main constituent features (e.g., decompose a topography into hill-like formations), or to identify transitions between different textural patterns [146].

The only areal partitioning method currently included in the ISO standard 25178-2 [83] is morphologic segmentation into hills or dales [142]. Morphologic segmentation is not intrinsically multiscale; however, the exploration of how segmentation results are influenced by the variation of Wolf- and area-pruning thresholds is a type of MSA, as pruning determines scale-related thresholds that control the merging of smaller partitions into larger ones. In 2003, Blunt and Jiang investigated how segmentation behavior varies in response to different Wolf-pruning thresholds [26], showing results for grit identification on the topography of a grinding wheel. In 2013, Senin et al. performed a similar analysis [145] by investigating the effects of varying Wolf- and area-pruning thresholds in the accuracy of boundary determination for a series of localized features (scratches on endoprostheses surfaces, elements of MEMS, and moles on human skin).

Berglund et al. [17,18] and Belaud et al. [16] performed systematic MACs on the effects of applying filters. Bandpass filtering was applied for the former (2010), and high- and lowpass, separately, for the latter (2015), at different wavelengths to the topography and before subjecting it to morphologic segmentation. These authors studied the effects on various ISO 25178-2 feature parameters (CPs resulting from morphological segmentation) and investigated their correlations with friction [17,18] and wetting [16].

Other segmentation methods natively include MAC: in 2007, Jiang et al. showed that wavelet decomposition of topographies, an intrinsically multiscale method, could be used for feature identification and provided examples of identification of scratches on the surface of replacement hip joints and identification of honing marks in plateau-honed surfaces [89]. In 2015, Senin et al. expanded the concept by introducing a general purpose segmentation and feature identification framework, where topographic properties useful for partitioning are extracted from multiscale decomposition, and illustrated the framework in operation by using wavelets, pyramid decompositions (Laplacian and Gaussian), and Gabor filter banks, all natively multiscale [147]. The framework was applied to identify elements of MEMS, moles on human skin, scratches on worn femoral heads, and grits on super-abrasive surfaces.

Another segmentation method, introduced by Senin et al. in 2007, consists of applying k-means multivariate clustering to identify regions where local texture properties are uniform enough and where there are transitions between such regions. Local texture properties were obtained by computing multiple CPs within a moving window [148]. The method was applied to the identification of micro-hardness indentations, firearm marks in cartridge cases, and grooves in scratch testing. Although segmentation with moving windows and multivariate clustering is not intrinsically multiscale, the authors did perform a systematic exploration of partitioning behavior when the size of the moving window varied, and with the application of different form-removal and filtering operators, thus identifying correlations between partitioning behavior and the window of wavelengths within which local topographic properties were computed.

### 5.7. Anisotropy

Anisotropy of surface texture can significantly influence the surface function in many practical cases. Tribological contacts in sheet forming and engine cylinder liners are typical examples. Anisotropy exists in a multiscale space and can vary with the scale of observation.

There are several methods available for analysis of texture anisotropy. In ISO 25178-2 [83], the two parameters Str (texture aspect ratio of the surface) and Std (texture direction of the surface) can be found (nonMCs). Str can vary from 0 to 1, where Str = 1 is isotropic, (similar in all directions) and Str = 0 is anisotropic (strong lay). Std is the dominant texture direction and can vary from 0 to 180° in regard to the coordinate system of the measurement (ISO 25178-2). These CPs are not multiscale by design. A way to use them as MCs is to first perform a MAC, e.g., through bandpass filtering, to create scale-limited datasets and then to calculate the CPs for each scale-limited data set.

In Berglund et al. [20], this approach was realized by constructing bandpass filters, combinations of high- and lowpass Gaussian filters (MAC), and, after filtering, computing the CPs Str, Sdr and Sq (root mean square height of the surface) at each scale, that is, for each bandpass filtered dataset (MCs). The objective was to demonstrate a method for the visualization of a number of surface texture properties related to the anisotropy of a surface in a single graph as a function of scale. The results were visualized in a 3D plot, as shown in Fig. 5.7.1, where strength and direction of anisotropy as well as texture height are shown for a finish-milled surface. To construct the 3D plot, a cylindrical surface was created using the function cyl3d in MATLAB, with the different levels of the cylinder representing different levels of scale. Two points were created at each level of scale in the plot. Both points were based on the same parameter values of Std and Str calculated for that scale. The coordinates for the points were (1-Str, Std) and (1-Str, Std + 180), respectively. 1-Str represents the distance from the center, and Std and Std + 180 are the angles. The purpose of having two points at each level instead of just one is that the symmetry will make the plot easier to interpret. For example, the texture directions 1° and 179° are very similar but could be misinterpreted as dissimilar, since they are directed in approxi-

mately opposite directions. Instead, with two symmetric points for each level and with the directions Std and Std + 180 the plot is clearer and easier to interpret. 1-Str was used instead of Str to create a plot where a strong anisotropy (low Str) would be shown more distinctly than a weak anisotropy. The Sq value for each scale was used to create a color bar.

In Thomas et al. [169], the 3D structure function was used for analysis of texture anisotropy on a number of surfaces. It was found that the fractal parameters are invariant with orientation for an isotropic surface; but, for a strongly anisotropic surface, the FD is the same in every direction, except parallel to the lay, while the topography changes dramatically. One of the example surfaces has a texture that is bifractal in scale, with different properties for the two wavelength bands.

In MAC of curvature tensors, principal directions of the maximum and minimum curvatures (MCSSs) can be determined. In Bartkowiak [8], the directions of the maximum were plotted for each location and scale. In addition, 2D and 3D distribution graphs were provided to visualize anisotropic or isotropic characteristics. This can be used to determine the dominant texture direction or directions for each scale. In contrast to conventional anisotropy determination techniques, such as Fourier transform or autocorrelation, the presented method provides the analysis in 3D and for every calculation location at each scale.

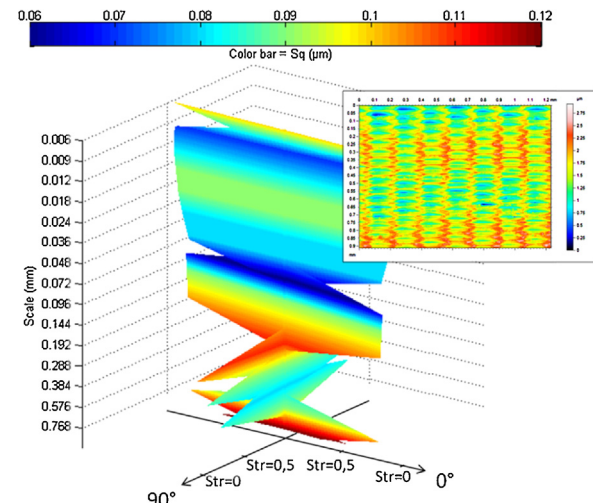


Fig. 5.7.1. Visualization of anisotropy at different scales. Inset, plot of the analyzed

Rosette plots have been used with fractals to study anisotropy. Chen et al. [58] show the anisotropy on machined optical surfaces, with the FD of profiles in different directions on milled and diamond turned surfaces of optical components. The MC length-scale has also been plotted in multiple directions [144,143]. The length of the normalized mean vector on the rosette was used as a measure of surface anisotropy, in order to distinguish different diets from microdental wear.

In Bartkowiak [8], the directions of the maximum curvatures (MCSS) were plotted for each location and scale. In addition, 2D and 3D distribution graphs were provided to visualize anisotropic or isotropic characteristics. This can be used to determine the dominant texture direction or directions for each scale. In contrast to conventional anisotropy determination techniques, such as Fourier transform or autocorrelation, the presented method provides the analysis in 3D and an analysis for every calculation location at each scale.

### 5.8. Modal projection for multiscale decomposition

A modal projection based on dynamics can be used to provide multiscale analyses and characterizations (MACs) of surface

topographies. The method, called Discrete Modal Decomposition (DMD), was initially implemented by Samper and Formosa [135] to characterize primary form variations [74] and, by filtering the primary form, to analyze waviness and roughness [102,77]. The DMD has also been implemented for outlier filtering of surface topographies [101].

DMD has been generalized to waviness and roughness by applying it with a constant low number of descriptors, typically 50, on a sliding window [100]. By progressively varying the width of the analysis window, this method is an MAC. An example of a multiscale application on a hot-rolled workpiece is presented in Fig. 5.8.1. The scale can thus be directly associated with the width of the sliding window.

This multiscale implementation of the DMD yields a compromise between the conventional and wavelet approaches to sliding bandpass filters. Indeed, it generally appears that the DMD method is relevant when the surface structure is not clearly periodic and presents complex surface structures, i.e., mixes of different surface topographic types. In the presence of localized defects, the wavelet approach is known to give results that are more relevant, even if the DMD method provides better performance than the conventional approach in these cases. This is because the modal-basis features yield modulated frequency and amplitude projection descriptors.

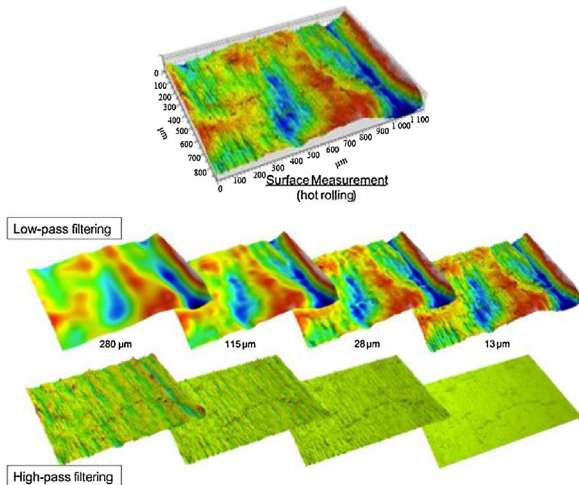


Fig. 5.8.1. Multiscale DMD application on a hot-rolled workpiece, from Ref. [100].

The scale decomposition operation projects the measured surface onto the modal basis, which is a free-form surface family composed by the structure eigenmodes (nonorthogonal basis of projection). The reference structure used for the modal-basis calculation is generally a plane, but the method can also be implemented with other geometry (cylinder, sphere, or hemisphere) to provide more relevant decomposition modes in specific applications. The surface to be characterized can thus be expressed as the sum of a linear combination of the modal vectors and the decomposition residual, as depicted in Eq. (5.8.1). Projection results can be represented in the form of a modal spectrum of amplitudes.

$$V = \sum_{i=1}^{N_q} \lambda_i Q_i + \varepsilon(N_q) \quad \text{with } \begin{cases} \lambda_i & \text{modal coordinates} \\ N_q & \text{number of mode of decomposition} \end{cases} \quad (5.8.1)$$

The DMD has other interesting features. Particularly, the expression of the surface as a sum of a linear combination of the modal vectors, as shown in Eq. (5.8.1), which characterizes the inspected surface in derivative spaces. The modes' derivative can be easily computed analytically or numerically [128], to build slope ( $D_x, D_y$ ) or curvature ( $K_{xx}, K_{xy}, K_{yy}$ ) modal bases. Then, the multiscale slope and curvature characterizations can be assessed

by associating the derivatives' modes to the modal coordinates calculated previously, when projecting the surface to be analyzed into the modal basis. A  $K_{xx}$  multiscale modal expression is given, as an example, in Eq. (5.7.2).

$$\begin{aligned} K_{xx,V} &= \frac{\partial^2 moe V}{\partial x^2} = \frac{\partial^2 (\sum_{i=1}^{N_q} \lambda_i Q_i)}{\partial x^2} + \frac{\partial^2 \varepsilon(N_q)}{\partial x^2} \\ &= \sum_{i=1}^{N_q} \lambda_i K_{xx,i} + \frac{\partial^2 \varepsilon(N_q)}{\partial x^2} \end{aligned} \quad (5.7.2)$$

## 6. Concluding remarks

Scale is the key that unlocks a dimension in which answers to scientific questions and solutions to engineering problems in surfaces topography can be sought through multiscale analyses and characterizations. To elucidate this dimension here, semantic, theoretical and philosophical frameworks have been proposed. Literature on applications has been reviewed. Commonly used multiscale methods have been compiled and described, and a system of categorization has been proposed.

### 6.1. Synthesis

There appear to be commonalities in the experimental works that show how to enhance the potential for surface metrology to provide value to industry, engineering and science. A few studies were able to find strong correlations between topographies and their processing or performance. Others found confident discriminations of topographies, according to the processing and performance. Both confident discrimination and strong correlations appear to be facilitated by using four things:

- Characterizations** that describe geometric features appropriate for the application, e.g., area for adhesion or mass transfer, and curvature for fatigue, both of which change with scale;
- Scales** fundamentally appropriate to the application that are indicated by regions in scale, often narrow, where there are high mean square ratios or regression coefficients;
- Statistics** appropriate for the application and phenomena, e.g., extreme values for fatigue, mean values for friction;
- Measurements** with adequate resolution in a range of scales that includes those scales fundamental to the phenomena of interest.

These four commonalities can be principles for the practice of surface metrology. These principles in turn can strengthen surface metrology as a scientific discipline, and help to move it beyond a mostly experiential discipline, currently defined largely by a collection of best practices and standards. Exploiting these four principles would enhance the possibility of providing new and improved understandings of topographically related phenomena.

Principles 2 and 4 are shown schematically in Fig. 6.1.1. If the required scales for understanding surface creation and behavior are not adequately represented in the measurement, they cannot be in the characterization. Additionally, if the characterizations are not appropriate to the application and if appropriate statistics are not applied then the functional correlations and discriminations will not be as strong or confident as they could be.

These new understandings would indicate the relations between topographies and phenomena. Relations that provide value by contributing to the solving of design problems. The relations would quantify functional-physical and process-physical relations, which compose design and process equations [164]. These equations enable evidence-based specifications and tolerancing of surface topographies in process and product design. These relations also facilitate quality assurance and process control for surface topographies.

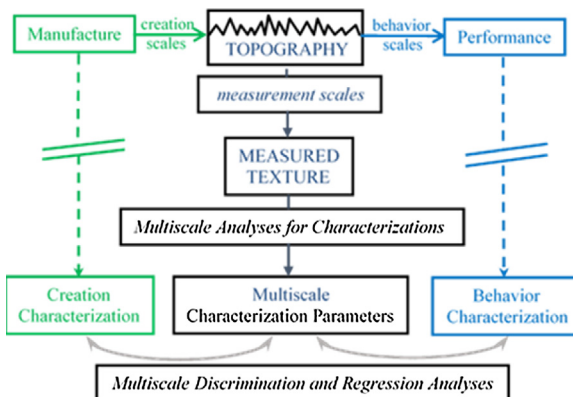


**Fig. 6.1.1.** Schematic for following scales in topographic studies.

These topography-phenomena relations are also valuable for solving problems in other fields, including forensics, paleontology, anthropology, geography, food science, and archaeology.

The disadvantage of multiscale analyses is that they require a higher level of sophistication and education than the relatively simplistic height parameters and traditional scale decomposition into roughness, waviness, and form. This disadvantage can be addressed through the development of better software for multiscale characterizations and analyses.

## 6.2. Future work and potential

Currently many more phenomena are suspected of influencing or being influenced by topographies than there is quantitative, experimental evidence for supporting these suspicions precisely and quantitatively. Multiscale analyses and characterizations in surface metrology provide a powerful means for discovering quantitative relations between topography and phenomena. In the next decade, more discoveries assisted by these multiscale methods should be appearing in the literature.

The lack of a system of characterizations, analyses and methods has handicapped research on topographically related phenomena [60]. The vast number of CPs have been critiqued for decades as creating 'confusion and expense' [188]. These critiques have discouraged the development of new parameters. New CPs should be welcomed if they add value by advancing the understanding of the relations between topographies and phenomena.

Improved systemization of the characterization and analysis methods for guiding research should be developed as well. Complete ontologies can further systemize the field of surface metrology and point the way to new CPs to complete systemizations, as in **Table 5.5.1**, for example.

There is a general tendency observed that the industry still uses mainly profile parameters to characterize the topographies they create or measure. On the other hand, there is a demand for new areal parameters for characterization of specific features [172]. Once areal measurements and new manufacturing techniques gain popularity, better education and guidance in good practice are required for surface texture parameters, allowing users to link surface texture parameters with process parameters and function, and better understand the parameter results and the information they give about the measured surface. MSA should provide this opportunity through correlation and discrimination using appropriate CPs. This could be facilitated by more intuitive, automated and easy-to-use software developed and widely distributed for industrial use. The main barrier in the broad application of multiscale methods is that the analysis is a complex and lengthy endeavor that requires more qualified personnel than the conventional surface texture analysis. Therefore, general expert systems that include conventional and multiscale methods would be highly appreciated.

New standards should be developed for multiscale analyses, to establish correlations and discriminations, and for the new CPs. These should result in more effective research and systematic advancement of surface metrology and improved, evidence-based specifications of topographies. Additionally comparisons of the methods on the same sets of data would be valuable additions to the literature.

These new developments in software and standards should help engineers and researchers to turn the key and unlock a new dimension for exploring for scientific discoveries and solutions to engineering problems.

## Acknowledgements

Enrico Savio, of the University of Padua, for contributing text and references and encouraging and insightful comments; John Ryan O'Neill, WPI '19 for assistance with the literature search; and Sheila McAvey, of Becker College, and Marilyn C. Brown for excellent editing; Karla Molina, WPI '19 for work on the figures, and support by Worcester Polytechnic Institute.

## References

- [1] Abdul-Rahman H, Jiang X, Scott P (2012) Freeform Surface Filtering Using the Lifting Wavelet Transform. *Precision Engineering* 37(1):187–202.
- [2] Aloisi V, Carmignato S (2016) Influence of Surface Roughness on X-ray Computed Tomography Dimensional Measurements of Additive Manufactured Parts. *Case Studies in Nondestructive Testing and Evaluation* 6:104–110.
- [3] Alvarez M, Fuentes NO, Favret EA, Vanina Dolce M, Forlano A (2012) Quantifying Use-wear Traces Through RIMAPS and Variogram Analyses. *Archaeological and Anthropological Sciences* 4:91–101.
- [4] ASME Standard, B46.1 (2009) *Surface Texture, Surface Roughness, Waviness and Lay*, American Society of Mechanical Engineers, New York, NY.
- [5] Astruc L, Vargiuoli R, Ben Tkaya M, Balkan-Atli N, Özbasaran Zahouani H (2012) Multiscale Tribological Analysis of the Technique of Manufacture of an Obsidian Bracelet from Asiki Höyük (Aceramic Neolithic, Central Anatolia). *Journal of Archaeological Science* 38(12):3415–3424.
- [6] Bar-On I, Brown CA (1995) Fractal Analysis of Fracture Surfaces Using the Patchwork Method. *Ceramic Transactions* 64:395–408.
- [7] Bar-On I, Brown CA, Johnsen WA, Calomino AM, Brewer DN (1996) Fractal Analysis of Fracture Surfaces using the Patchwork Method, Ceramic Transactions, 64. in Varner JP, Frechette VD, Quinn GD, (Eds.) *Third Alfred Conference on Fractography of Glasses and Ceramics*, Am. Ceramic Soc., Westerville, OH395–408.
- [8] Bartkowiak T (2017) Characterization of 3D Surface Texture Directionality Using Multiscale Curvature Tensor Analysis. *Proceedings of the ASME 2017 International Mechanical Engineering Congress and Exposition IMECE17*, November 3–9, 2017, Tampa, Florida, USA paper IMECE2017-71609.
- [9] Bartkowiak T, Berglund J, Brown CA (2017) Establishing Functional Correlations Between Multiscale Areal Curvature and Coefficient of Friction for Machined Surfaces. *16th International Conference on Metrology and Properties of Engineering Surfaces*, Gothenburg, Sweden paper P20.
- [10] Bartkowiak T, Brown C (2016) Multiscale Curvature Tensor Analysis of Machined Surfaces. *Archives of Mechanical Technology and Materials* 36:1–7.
- [11] Bartkowiak T, Brown CA (2018) A Characterization of Process-Surface Texture Interactions in Micro-Electrical Discharge Machining Using Multiscale Curvature Tensor Analysis. *Journal of Manufacturing Science and Engineering* 140 (2):021013.
- [12] Bartkowiak T, Hyde J, Brown CA (2016) Multiscale Curvature Tensor Analysis of Surfaces Created by Micro-EDM and Functional Correlations with Discharge Energy. *5th International Conference on Surface Metrology*, Poznan University of Technology, Poznan, Poland.
- [13] Bartkowiak T, Lehner JT, Hyde J, Wang Z, Pedersen DB, Hansen HN, Brown CA (2015) Multiscale Areal Curvature Analysis of Fused Deposition Surfaces. *ASPE Spring Topical Meeting on Achieving Precision Tolerances in Additive Manufacturing*, Raleigh, North Carolina.
- [14] Bartkowiak T, Staniak R (2016) Application of Multiscale Areal Curvature Analysis to Contact Problem, Insights and Innovations in Structural Engineering, Mechanics and Computation. *Proceedings of the 6th International Conference on Structural Engineering Mechanics and Computation SEMC 2016*:1823–1829.
- [15] Bartscher M, Hilpert U, Goebels J, Weidemann G (2007) Enhancement and Proof of Accuracy of Industrial Computed Tomography (CT) Measurements. *Annals of the CIRP Manufacturing Technology* 56(1):495–498.
- [16] Belaud V, Valette S, Stremsdoerfer G, Bigerelle M, Benayoun S (2015) Wettability versus Roughness: Multiscales Approach. *Tribology International* 82:343–349.
- [17] Berglund J, Agunwamba C, Powers B, Brown CA, Rosén B-G (2010) On Discovering Relevant Scales in Surface Roughness Measurement—An Evaluation of a Band-Pass Method. *Scanning* 32:244–249.
- [18] Berglund J, Brown CA, Rosén B-G, Bay N (2010) Milled Die Steel Surface Roughness Correlation with Steel Sheet Friction. *Annals of the CIRP Manufacturing Technology* 59(1):577–580.

- [19] Berglund J, Liljengren M, Rosén B-G (2011) On Finishing of Pressing Die Surfaces Using Machine Hammer Peening. *The International Journal of Advanced Manufacturing Technology* 52(1–4):115–121.
- [20] Berglund J, Wiklund D, Rosén BG (2011) A Method for Visualization of Surface Texture Anisotropy in Different Scales of Observation. *Scanning* 33(5):325–331.
- [21] Bigerelle M, Mathia T, Bouvier S (2012) The Multiscale Roughness Analyses and Modeling of Abrasion with the Grit Size Effect on Ground Surfaces. *Wear* 286:124–135.
- [22] Bigerelle M, Mazeran PE, Gong W, Giljean S, Anselme K (2011) A Method to Determine the Spatial Scale Implicated in Adhesion. Application on Human Cell Adhesion on Fractal Isotropic Rough Surfaces. *The Journal of Adhesion* 87 (7–8):644–670.
- [23] Bigerelle M, Van Gorp A, Iost A (2008) Multiscale roughness analysis in injection-molding process. *Polymer Engineering & Science* 48(9):1725–1736.
- [24] Bitton E, Marmur A (2012) The Role of Multiscale Roughness in the Lotus Effect: Is It Essential for Super-hydrophobicity? *Langmuir* 28(39):13933–13942.
- [25] Blateyron F (2017) New Generation of Sliding Band-pass Filters for the Multi-scale Exploration of Surface Texture. *16th International Conference on Metrology and Properties of Engineering Surfaces*. poster.
- [26] Blunt L, Jiang X (2003) *Numerical Parameters for Characterisation of Topography, Advanced Techniques for Assessment Surface Topography*, Kogan Page Science, Oxford17–41.
- [27] Borri-Brunetto M, Chiaia B, Ciavarella M (2001) Incipient Sliding of Rough Surfaces in Contact: A Multiscale Numerical Analysis. *Computer Methods in Applied Mechanics and Engineering* 190(46):6053–6073.
- [28] Boryczko A (2013) Effect of Waviness and Roughness Components on Transverse Profiles of Turned Surfaces. *Measurement* 46(1):688–696.
- [29] Braatz RD, Alkire RC, Seebauer E, Rusli E, Gunawan R, Drews TO, Li X, He Y (2006) Perspectives on the Design and Control of Multiscale Systems. *Journal of Process Control* 16(3):193–204.
- [30] Briones V, Brown CA, Aguilera JM (2006) Effect of Surface Topography on Color and Gloss of Chocolate Samples. *Journal of Food Engineering* 77(4):776–783.
- [31] Brown CA (1994) Concurrent Design of Engineering Surfaces Using Patchwork Analysis. *Fractals* 2(3):423–442.
- [32] Brown CA (1994) A Method for Concurrent Engineering Design of Chaotic Surface Topographies. *Journal of Materials Processing Technology* 44:337–344.
- [33] Brown CA (2000) In Tate D, (Ed.) *Axiomatic Design of Chaotic Components of Surface Textures, ICAD2000*, Institute for Axiomatic Design, Cambridge106–111.
- [34] Brown CA (2011) Axiomatic Design Applied to a Practical Example of the Integrity of Shaft Surfaces for Rotating Lip Seals. *1st CIRP Conference on Surface Integrity (CSI)*, 19. 53–59.
- [35] Brown CA, Bergstrom TS, Nucifora KA (2000) Upper Envelopes in Scale-series on Profiles. In Dietzsch M, Trumppold H, (Eds.) *Proceedings of the 10th International Colloquium of Surfaces Chemnitz*, 360–366Shaker Verlag, Aachen.
- [36] Brown CA, Charles PD, Johnsen WA, Chesters S (1993) Fractal Analysis of Topographic Data by the Patchwork Method. *Wear* 161(1–2):61–67.
- [37] Brown CA, Etievant D, Shao Y, Storie Nevers S, Bartkowiak T (2017) Multiscale Outlier Filtering with Curvature and Higher Spatial Finite Differences. *16th International Conference on Metrology and Properties of Engineering Surfaces*, Gothenburg, Sweden.
- [38] Brown, CA, Etievant, D, Shao, Y, Nevers, S, Bartkowiak. T (2017) Measurement Equipment with Outlier Filter, U.S. Patent App. No. 15/670, 533, filed Aug. 7, 2017.
- [39] Brown CA, Hahn RS St, Gelais RM, Powers B, Geiger DJ (2007) Grinding Wheel Texture and Diamond Roll Plunge Dressing Feed-Rates. *ISAT 2007/SME International Grinding Conference, Society of Manufacturing Engineers*, Dearborn, MI.
- [40] Brown CA, Johnsen WA, Butland RM (1996) Scale-sensitive Fractal Analysis of Turned Surfaces. *Annals of the CIRP – Manufacturing Technology* 45(1):515–518.
- [41] Brown, CA, Johnsen, WA, Charles, PD (1994) Method of Quantifying the Topographic Structure of a Surface. U.S. Patent 5, 307, 292.
- [42] Brown CA, Johnsen WA, Hult KM (1998) Scale-sensitivity, Fractal Analysis and Simulations. *International Journal of Machine Tools and Manufacturing* 38(5–6):633–637.
- [43] Brown CA, Nucifora KA, Luchini M, Bergstrom TS (1998) New Tiling and Packing Algorithms in Surface Metrology. *Proceedings, 14th Annual Meeting, The American Society for Precision Engineering*, St. Louis, ASPE, Raleigh, NC.
- [44] Brown CA, Savary G (1991) Describing Ground Surface Texture using Contact Profilometry and Fractal Analysis. *Wear* 141:211–226.
- [45] Brown CA, Shipulski EM (1994) Concurrent Engineering Design of Surface Roughness using Scale-area Analysis, ASME Production Engineering Division, PED 68/1. *Manufacturing Science and Engineering* 155–160.
- [46] Brown CA, Siegmund S (2001) Fundamental Scales of Adhesion and Area-scale Fractal Analysis. *International Journal of Machine Tools and Manufacture* 41 (13):1927–1933.
- [47] Brown, CA, Wang, Z, Lehner, JT, Pedersen, DB, Hansen, HN (2017) Fused Deposition ABS Surface Discrimination with Angle and Acetone Polishing, in press.
- [48] Bruzzone AAG, Costa HL, Lonardo PM, Lucca DA (2008) Advances in Engineered Surfaces for Functional Performance. *Annals of the CIRP – Manufacturing Technology* 57(2):750–769.
- [49] Burgman JHE, Leichtliter J, Avenant NL, Ungar PS (2016) Dental Microwear of Sympatric Rodent Species Sampled Across Habitats in Southern Africa: Implications for Environmental Influence. *Integrative Zoology* 11 (2):111–127.
- [50] Burns CM, Brown CA (2014) Form and Outlier Removal by Modal Filtering of Confocal Measurement of Laser-sintered Additive-manufactured Surfaces. *29th Annual Meeting of the American Society for Precision Engineering*.
- [51] Calandra I, Schulz E, Pinnow M, Krohn S, Kaiser TM (2012) Teasing Apart the Contributions of Hard Dietary Items on 3D Dental Microtextures in Primates. *Journal of Human Evolution* 63(1):85–98.
- [52] Cantor GJ, Brown CA (2009) Scale-based Correlations of Relative Areas with Fracture of Chocolate. *Wear* 266(5):609–612.
- [53] Caporale SS, Ungar PS (2016) Rodent Incisor Microwear as a Proxy for Ecological Reconstruction. *Palaeogeogr Palaeoecol* 446:225–233.
- [54] Carmignato S (2012) Accuracy of Industrial Computed Tomography Measurements: Experimental Results from an International Comparison. *Annals of the CIRP – Manufacturing Technology* 61(1):491–494.
- [55] Carmignato S, Dreossi D, Mancini L, Marinello F, Tromba G, Savio E (2009) Testing of X-ray Microtomography Systems using a Traceable Geometrical Standard. *Measurement Science & Technology* 20084021. ISSN: 0957-0233.
- [56] Carmignato S, Savio E (2011) Traceable Volume Measurements Using Coordinate Measuring Systems. *Annals of the CIRP Manufacturing Technology* 60 (1):519–522. ISSN: 0007-8506.
- [57] Chegdnai F, Mezghani S, El Mansori M (2016) Correlation Between Mechanical Scales and Analysis Scales of Topographic Signals under Milling Process of Natural Fibre Composites. *Journal of Composite Materials* 51(19):2743–2756.
- [58] Chen M, Pang Q, Wang J, Cheng K (2008) Analysis of 3D Microtopography in Machined KDP Crystal Surfaces Based on Fractal and Wavelet Methods. *International Journal of Machine Tools and Manufacture* 48(7):905–913.
- [59] Cui FZ, Ge J (2007) New Observations of the Hierarchical Structure of Human Enamel, from Nanoscale to Microscale. *Journal of Tissue Engineering and Regenerative Medicine* 1(3):185–191.
- [60] Das J, Linke B (2017) Evaluation and Systematic Selection of Significant Multi-scale Surface Roughness Parameters (SRPs) as Process Monitoring Index. *Journal of Materials Processing Technology* 244:157–165.
- [61] Daw DF, Brown CA, van Griethuysen JP, Albert JFLM (1990) Surface Topography Investigations by Fractal Analysis of Spark Eroded Electrically Conductive Ceramics. *Annals of the CIRP – Manufacturing Technology* 39(1):161–165.
- [62] De Chiffre L, Carmignato S, Kruth JP, Schmitt R, Weckenmann A (2014) Industrial Applications of Computed Tomography. *Annals of the CIRP – Manufacturing Technology* 63(2):655–677.
- [63] De Chiffre L, Kunzmann H, Peggs GN, Lucca DA (2003) Surfaces in Precision Engineering, Microengineering and Nanotechnology. *Annals of the CIRP – Manufacturing Technology* 52(2):561–577.
- [64] De Chiffre L, Lonardo P, Trumppold HDA, Goch G, Brown CA, Raja J, Hansen HN (2000) Quantitative Characterisation of Surface Texture. *Annals of the CIRP – Manufacturing Technology* 49(2):635–652.
- [65] Delezeni L, Teaford MF, Ungar PS (2016) Canine and Incisor Microwear in Pitheciids and Atelids Reflects Documented Patterns of Tooth Use. *American Journal of Physical Anthropology* 161(1):6–25.
- [66] DeSantis LRG (2016) Dental Microwear Textures: Reconstructing Diets of Fossil Mammals. *Surface Topography: Metrology and Properties* 4023002.
- [67] Dixon B, Earls J (2009) Resample or not? Effects of Resolution of DEMs in Watershed Modeling. *Hydrological Processes* 23(12):1714–1724.
- [68] Dixon B, Uddameri V, Ray C (2015) *GIS and Geocomputation for Water Resource Science and Engineering*, John Wiley & Sons, Hoboken NJ.
- [69] Donohue SL, DeSantis LRG, Schubert BW, Ungar PS (2013) Was the Giant Short-faced Bear a Hyper-scavenger? A New Approach to the Dietary Study of Ursids Using Dental Microwear Textures. *PLoS One* 8(10).
- [70] Emerson IV RJ, Bergstrom TS, Liu Y, Soto ER, Brown CA, McGimpsey WG, Camessano TA (2006) Microscale Correlation Between Surface Chemistry, Texture, and the Adhesive Strength of *Staphylococcus epidermidis*. *Langmuir* 22(26):11311–11321.
- [71] Evans AA (2014) On the Importance of Blind Testing in Archaeological Science: The Example from Lithic Functional Studies. *Journal of Archaeological Science* 48:5–14.
- [72] Favret EA, Fuentes NO, Álvarez MR (2004) RIMAPS and Variogram Analyses of Microwear Traces in Experiments with Stone Tools. *Microscopy and Microanalysis* 10(Suppl. 2):968–969.
- [73] Ferrucci M, Leach RK, Giusca C, Carmignato S, Dewulf W (2015) Towards Geometrical Calibration of X-ray Computed Tomography Systems—A Review. *Measurement Science and Technology* 26(9):092003.
- [74] Formosa F, Samper S, Perpoli I (2005) Modal Expression of Form Defects. *Proceedings of the 9th CIRP Seminar on Models for Computer Aided Tolerancing* 1–9.
- [75] Gao G (1997) Resolution and Accuracy of Terrain Representation by Grid DEMs at a Micro-scale. *International Journal of Geographical Information Science* 11 (2):199–212. <http://dx.doi.org/10.1080/136588197242464>.
- [76] Gleason MA, Kordell S, Lemoine A, Brown CA (2013) Profile Curvatures by Heron's Formula as a Function of Scale and Position on an Edge Rounded by Mass Finishing. *14th International Conference on Metrology and Properties of Engineering Surfaces*, Taipei, Taiwanpaper TS4-01, 0022.
- [77] Grandjean J, Le Gorc G, Favreliere H, Ledoux Y, Samper S, Formosa F, Devun L, Gradel T (2012) Multi-scalar Analysis of Hip Implant Components Using Modal Decomposition. *Measurement Science and Technology* 23(12):125702.
- [78] Grine FE, Ungar PS, Teaford MF (2002) Error Rates in Dental Microwear Quantification Using Scanning Electron Microscopy. *Scanning* 24(3):144–153.
- [79] Hani A, Sathyamoorthy D, Asirvadam V (2011) A Method for Computation of Surface Roughness of Digital Elevation Model Terrains via Multiscale Analysis. *Computers & Geosciences* 37(2):177–192.
- [80] Haupt RJ, DeSantis LRG, Green JL, Ungar PS (2013) Dental Microwear Texture as a Proxy for Diet in Xenarthrans. *Journal of Mammalogy* 94(4):856–866.
- [81] He LH, Swain MV (2008) Understanding the Mechanical Behaviour of Human Enamel from its Structural and Compositional Characteristics. *Journal of the Mechanical Behavior of Biomedical Materials* 1(1):18–29.
- [82] Hyde JM, Cadet L, Montgomery J, Brown CA (2014) Multiscale Areal Topographic Analysis of Surfaces Created by Micro-EDM and Functional Correla-

- tions with Discharge Energy. *Surface Topography: Metrology and Properties* 2(4):045001.
- [83] ISO 25178-2. *Geometrical product specifications (GPS)—Surface texture: Areal—Part 2*.
- [84] Jiang X, Abdul-Rahman H, Scott P (2013) Multiscale Freeform Surface Texture Filtering Using a Mesh Relaxation Scheme. *Measurement Science and Technology* 24(11):115001.
- [85] Jiang X, Blunt L, Stout K (1999) Three-dimensional Surface Characterization for Orthopaedic Joint Prostheses. *Proceedings of the Institution of Mechanical Engineers Part H: Journal of Engineering in Medicine* 213(1):49–68.
- [86] Jiang X, Blunt L, Stout K (2000) Development of a Lifting Wavelet Representation for Characterisation of Surface Topography. *Proceedings of the Royal Society London A* 456:1–31.
- [87] Jiang X, Blunt L (2001) Morphological Assessment of in Vivo Wear of Orthopedic Implants Using Multiscale Wavelets. *Wear* 250(1–12):217–221.
- [88] Jiang X, Blunt L (2004) Third Generation Wavelet for the Extraction of Morphological Features from Micro and Nano Scalar Surfaces. *Wear* 257:1235–1240.
- [89] Jiang X, Scott P, Whitehouse D, Blunt L (2007) Paradigm Shifts in Surface Metrology, Part II: The Current Shift. *Proceedings of the Royal Society London A* 463(2085):2071–2099.
- [90] Jiang X, Zeng W, Scott P, Ma J, Blunt L (2008) Linear Feature Extraction Based on Complex Ridgelet Transform. *Wear* 264(5–6):428–433.
- [91] Jiang XJ, Whitehouse DJ (2012) Technological Shifts in Surface Metrology. *Annals of the CIRP – Manufacturing Technology* 61(2):815–836.
- [92] Jing C, Tang W (2016) Ga-doped ZnO Thin Film Surface Characterization by Wavelet and Fractal Analysis. *Applied Surface Science* 364:843–849.
- [93] Jordan SE, Brown CA (2006) Comparing Texture Characterization Parameters on Their Ability to Differentiate Ground Polyethylene Ski Bases. *Wear* 261:398–409.
- [94] Karabelchikova O, Brown CA, Sisson Jr RD. (2007) Effect of Surface Roughness on Kinetics of Mass Transfer During Gas Carburizing. *International Heat Treatment and Surface Engineering* 1(4):164–170.
- [95] Karabelchikova O, Brown CA, Sisson Jr RD. (2008) Effect of Surface Roughness on the Kinetics of Mass Transfer During Gas Carburizing. *HTM Journal of Heat Treatment and Materials* 63(5):257–264. (formerly HTM Z. Werkst, Warnebeck, Fertigung).
- [96] Kennedy FE, Brown CA, Kolodny J, Sheldon BM (1999) Fractal Analysis of Hard Disk Surface Roughness and Correlation with Static and Low-speed Friction. *ASME Journal of Tribology* 121(4):968–974.
- [97] Key AJM, Stemp WJ, Morozov M, Proffitt T, de la Torre I (2015) Is Loading a Significantly Influential Factor in the Development of Lithic Microwear? An Experimental Test Using LSCM on Basalt from Olduvai Gorge. *Journal of Archaeological Method and Theory* 22(4):1193–1214.
- [98] Kruth JP, Bartscher M, Carmignato S, Schmitt R, De Chiffre L, Weckenmann A (2011) Computed Tomography for Dimensional Metrology. *Annals of the CIRP – Manufacturing Technology* 60(2):821–842.
- [99] Lavernhe S, Quinsat Y, Lartigue C, Brown CA (2014) Realistic Simulation of Surface Defects in 5-axis Milling Using the Measured Geometry of the Tool. *International Journal of Advanced Manufacturing Technology* 74:393–401. <http://dx.doi.org/10.1007/s00170-014-5689-7>.
- [100] Le Goïc G, Bigerelle M, Samper S, Favrelière H, Pillet M (2016) Multiscale Roughness Analysis of Engineering Surfaces: A Comparison of Methods for the Investigation of Functional Correlations. *Mechanical Systems and Signal Processing* 66:437–457.
- [101] Le Goïc G, Brown CA, Favrelière H, Samper S, Formosa F (2013) Outlier Filtering: A New Method for Improving the Quality of Surface Measurements. *Measurement Science and Technology* 24(1):015001.
- [102] Le Goïc G, Favrelière H, Samper S, Formosa F (2011) Multi Scale Modal Decomposition of Primary Form, Waviness and Roughness of Surfaces. *Scanning The Journal of Scanning Microscopies* 33:332–341. (Special Issue on Surface Metrology II).
- [103] Le Goïc G, Samper S (2014) Modal Curvature Estimation: a Multiscale Approach for Surface Topography. *International Conference on Surface Topography ICSM 2014*, HamburgPublication in progress.
- [104] Lemoine AC, Mancini MP, Velez JA, Brown CA (2016) On the Metrology of Surfaces Produced by Laser Melting of Powders. *ASPE, Topical Meeting Dimensional Accuracy and Surface Finish in Additive Manufacturing*, June 27–30, Raleigh, North Carolina.
- [105] Lee SH, Zahouani H, Caterini R, Mathia TG (1998) Morphological Characterization of Engineered Surfaces by Wavelet Transform. *International Journal of Machine Tools and Manufacturing* 38(5–6):581–589.
- [106] Lesnik JJ (2011) Bone Tool Texture Analysis and the Role of Termites in the Diet of South African Hominids. *Paleoanthropology* 11:268–281.
- [107] Lifton JJ, Carmignato S (2017) Simulating the Influence of Scatter and Beam Hardening in Dimensional Computed Tomography. *Measurement Science and Technology* 28(10).
- [108] Liu S, Zhao J, Qin WZ, Pang JM (2016) Effect of Spindle Speeds on 3D Topography of Ball-End Milled Surfaces Using Wavelet Analysis Method. *Materials Science Forum* 836(37):13–19.
- [109] Lonardo PM, Trampold H, De Chiffre L (1996) Progress in 3D Surface Microtopography Characterization. *Annals of the CIRP—Manufacturing Technology* 45(2):589–598.
- [110] Lovejoy S (1982) Area-perimeter Relation for Rain and Cloud Areas. *Science* 216(4542):185–187.
- [111] Lou S, Abdou H, Zeng W, Jiang X, Paul S (2017) A Preliminary Investigation on Surface Roughness Assessment of Complex Additive Manufactured Parts Scanned by X-ray Computed Tomography. *7th Conference on Industrial Computed Tomography February 7–9, 2017, Leuven, Belgium*.
- [112] Magritte R (1929) La trahison des images, Los Angeles County Museum of Art.
- [113] Malchiodi MC, Brown CA (2000) Area-scale Analysis for Understanding Fracture Energy, Metrology and Properties of Engineering Surfaces. *8th International Conference, April 26–28, 2000, Huddersfield, England*.
- [114] Malshe A, Rajurkar K, Samant A, Hansen HN, Bapat S, Jiang W (2013) Bio-inspired Functional Surfaces for Advanced Applications. *Annals of the CIRP—Manufacturing Technology* 62(2):607–628.
- [115] Mandelbrot BB (1967) How Long is the Coast of Britain. *Science* 156(3775):636–638.
- [116] Mandelbrot BB (1982) *The Fractal Geometry of Nature*, W.H Freeman and Co., San Francisco, CA.
- [117] Mandelbrot BB (2012) *The Fractalist: Memoir of a Scientific Maverick*, Vintage, New York, NY.
- [118] McRae GA, Maguire MA, Jeffrey CA, Guzonas DA, Brown CA (2002) Atomic Force Microscopy of Fractal Anodic Oxides on Zr-2.5Nb. *Journal of Applied Surface Science* 191(1–4):94–105.
- [119] Meirose L, Dixon B, Brown CA (2018) *Multiscale Analysis of the Effects of DEM Resolution on Fractal Complexity and Subsequent Flow Direction, Accumulation and Stream Definition*, American Association of Geographers April 10–14, 2018.
- [120] Merceron G, Escarguel G, Angibault JM, Verheyden-Tixier H (2010) Can Dental Microwear Textures Record Inter-individual Dietary Variations? *PLoS One* 5(3).
- [121] Merceron G, Hofman-Kaminska E, Kowalczyk R (2014) 3D Dental Microwear Texture Analysis of Feeding Habits of Sympatric Ruminants in the Bialowieza Primeval Forest, Poland. *Forest Ecology and Management* 328:262–269.
- [122] Mezghani S, Zahouani H, Piezanowski JJ (2011) Multiscale Characterizations of Painted Surface Appearance by Continuous Wavelet Transform. *Journal of Materials Processing Technology* 211(2):205–211.
- [123] Mezghani S, El Mansori M, Massaq A, Ghidossi P (2008) Correlation Between Surface Topography and Tribological Mechanisms of the Belt-finishing Process Using Multiscale Finishing Process Signature. *Comptes Rendus Mécanique* 336(10):794–799.
- [124] Moreno MC, Brown CA, Bouchon P (2010) Effect of Food Surface Roughness on Oil Uptake by Deep-fat Fried Products. *Journal of Food Engineering* 101:179–186.
- [125] Narayan P, Hancock BC, Hamel R, Bergstrom TS, Childs BE, Brown CA (2006) Differentiation of the Surface Topographies of Pharmaceutical Excipient Compacts. *Materials Science and Engineering: A* 430(1):79–89.
- [126] Pitard G, Le Goïc G, Mansouri A, Favrelière H, Desage SF, Samper S, Pillet M (2017) Discrete Modal Decomposition: A New Approach for the Reflectance Modeling and Rendering of Real Surfaces. *Machine Vision and Applications* 28:607–621.
- [127] Podsiadlo P, Wolski M, Stachowiak GW (2017) Novel Directional Blanket Covering Method for Surface Curvature Analysis at Different Scales and Directions. *Tribology letters* 65(1):2.
- [128] Pottier T, Louche H, Samper S, Favrelière H, Toussaint F, Vacher P (2014) Proposition of a Modal Filtering Method to Enhance Heat Source Computation within Heterogeneous Thermomechanical Problems. *International Journal of Engineering Science* 81:1–14.
- [129] Power WL, Durham WB (1997) Topography of Natural and Artificial Fractures in Granitic Rocks: Implications for Studies of Rock Friction and Fluid Migration. *International Journal of Rock Mechanics and Mining Sciences* 34(6):979–989.
- [130] Prideaux GJ, Alyiffe LK, DeSantis LRG, Schubert BW, Murray PF, Gagan MK, Cerling TE (2009) Extinction Implications of a Chenopod Browse Diet for a Giant Pleistocene Kangaroo. *Proceedings of the National Academy of Sciences* 106(28):11646–11650.
- [131] Purnell MA, Crumpton N, Gill PG, Jones G, Rayfield EJ (2013) Within-guild Dietary Discrimination from 3-D Textural Analysis of Tooth Microwear in Insectivorous Mammals. *Journal of Zoology* 291(4):249–257.
- [132] Quinsat Y, Lartigue C, Brown CA, Hattali L (2017) Multiscale Surface Characterization in Additive Manufacturing Using CT. *Advances on Mechanics, Design Engineering and Manufacturing*, Springer International Publishing: 271–280.
- [133] Rosén B-G, Ohlsson R, Thomas TR (1998) Nano Metrology of Cylinder Bore Wear. *International Journal of Machine Tools and Manufacture* 38(5–6):519–527.
- [134] Sabri L, Mezghani S, El Mansori M, Zahouani H (2011) Multiscale Study of Finish-honing Process in Mass Production of Cylinder Liner. *Wear* 271(3–4):509–513.
- [135] Samper S, Formosa F (2007) Form Defects Tolerancing by Natural Modes Analysis. *Journal of Computing and Information Science in Engineering* 7(1):44–51.
- [136] Sayles RS, Thomas TR (1977) The Spatial Representation of Surface Roughness by Means of the Structure Function: A Practical Alternative to Correlation. *Wear* 42:263–276.
- [137] Schubert BW, Ungar PS, DeSantis LRG (2010) Carnassial Microwear and Dietary Behaviour in Large Carnivorans. *Journal of Zoology* 280:257–263.
- [138] Schulz E, Calandra I, Kaiser TM (2010) Applying Tribology to Teeth of Hoofed Mammals. *Scanning* 32(4):162–182.
- [139] Scott JR (2012) Dental Microwear Texture Analysis of Extant African Bovidae. *Mammalia* 76(2):157–174.
- [140] Scott PJ (2004) Pattern Analysis and Metrology: The Extraction of Stable Features from Observable Measurements. *Proceedings of the Royal Society London A* 460:2845–2864.
- [141] Scott PJ, Jiang X (2014) Freeform Surface Characterisation: Theory and Practice. *Journal of Physics: Conference Series* 483(No. 1):012005. IOP Publishing.
- [142] Scott PJ (2004) Pattern Analysis and Metrology: The Extraction of Stable Features from Observable Measurements. *Proceedings of the Royal Society London A* 460:2845–2864.

- [143] Scott RS, Teaford MF, Ungar PS (2012) Dental Microwear Texture and Anthropoid Diets. *American Journal of Physical Anthropology* 147(4):551–579.
- [144] Scott RS, Ungar PS, Bergstrom TS, Brown CA, Grine FE, Teaford MF, Walker A (2005) Dental Microwear Texture Analysis Within-species Diet Variability in Fossil Hominins. *Nature* 436(4):693–695.
- [145] Senin N, Blunt L (2013) Characterisation of Individual Areal Features. In Leach RK, (Ed.) *Characterisation of Areal Surface Texture*, Springer, Heidelberg 179–216.
- [146] Senin N, Blunt LA, Leach RK, Pini S (2013) Morphologic Segmentation Algorithms for Extracting Individual Surface Features from Areal Surface Topography Maps. *Surface Topography: Metrology and Properties* 1(1):15005.
- [147] Senin N, Leach R, Pini S, Blunt L (2015) Texture-based Segmentation with Gabor Filters, Wavelet and Pyramid Decompositions for Extracting Individual Surface Features from Areal Surface Topography Maps. *Measurement Science and Technology* 26(9):095405.
- [148] Senin N, Ziliotti M, Gropetti R (2007) Three-dimensional Surface Topography Segmentation Through Clustering. *Wear* 262(3–4):395–410.
- [149] Shipulski EM, Brown CA (1994) A scale-based Model of Reflectivity. *Fractals* 2/03:413–416.
- [150] Souron A, Merceron G, Blondel C, Brunetiere N, Colyn M, Hofman-Kaminska E, Boissiere JR (2015) Three-Dimensional Dental Microwear Texture Analysis and Diet in Extant Suidae (Mammalia: Cetartiodactyla). *Mammalia* 79(3):279–291.
- [151] Spartacusa V, Vargiolud R, Zahouani H, Nemoz-Gaillard M, Chabrand P (2017) Multi-scale analysis of cartilage surface for trapeziometacarpal hemi-arthroplasty. *Biosurface and Biotribology* 3(2):45–55.
- [152] Stach S, Cybo J, Chmiela J (2001) Fracture Surface—fractal or Multifractal? *Materials Characterization* 46(2):163–167.
- [153] Stemp WJ (2014) A Review of Quantification of Lithic Use-wear Using Laser Profilometry: a Method Based on Metrology and Fractal Analysis. *Journal of Archaeological Science* 48:15–25.
- [154] Stemp WJ, Andruskiewicz MD, Gleason MA, Rashid YH (2015) Experiments in Ancient Maya blood-letting: Quantification of Surface Wear on Obsidian Blades. *Archaeological and Anthropological Sciences* 7(4):423–439.
- [155] Stemp WJ, Childs BE, Vionnet S (2010) Laser Profilometry and Length-scale Analysis of Stone Tools: Second Series Experiment Results. *Scanning* 32:233–243.
- [156] Stemp WJ, Childs BE, Vionnet S, Brown CA (2009) Quantification and Discrimination of Lithic Use-wear: Surface Profile Measurements and Length-scale Fractal analysis. *Archaeom* 51:366–382.
- [157] Stemp WJ, Chung S (2011) Discrimination of Surface Wear on Obsidian Tools Using LSCM and RelA: Pilot Study Results. *Scanning* 33:279–293.
- [158] Stemp WJ, Lerner HJ, Kristant EH (2013) Quantifying Microwear on Experimental Mistassini Quartzite Scrapers: Preliminary Results of Exploratory Research Using LSCM and Scale-sensitive Fractal Analysis. *Scanning* 35:28–39.
- [159] Stemp WJ, Lerner HJ, Kristant EH (2017) Testing Area-Scale Fractal Complexity (Asfc) and Laser Scanning Confocal Microscopy (LSCM) to Document and Discriminate Microwear on Experimental Quartzite Scrapers. *Archaeometry*.
- [160] Stemp WJ, Morozov M, Key AJM (2015) Quantifying Lithic Microwear with Load Variation on Experimental Basalt Flakes Using LSCM and Area-scale Fractal Complexity (Asfc). *Surface Topography: Metrology and Properties* 3(3):1–20.
- [161] Stemp WJ, Stemp M (2001) UBM Laser Profilometry and Lithic Use-wear Analysis: A Variable Length Scale Investigation of Surface Topography. *Journal of Archaeological Science* 28:81–88.
- [162] Stemp WJ, Stemp M (2003) Documenting Stages of Polish Development on Experimental Stone Tools: Surface Characterization by Fractal Geometry Using UBM Laser Profilometry. *Journal of Archaeological Science* 30:287–296.
- [163] Stemp WJ, Watson AS, Evans AA (2016) Surface Analysis of Stone and Bone Tools. *Surface Topography: Metrology and Properties* 4(1):1–25.
- [164] Suh NP (1990) *Principles of Design*, Oxford University Press, on demand.
- [165] alu S, Stach S, Mahajan A, Pathak D, Wagner T, Kumar A, Bedi RK (2014) Multifractal Analysis of Drop-casted Copper(II) Tetrasulfophthalocyanine Film Surfaces on the Indium Tin Oxide Substrates. *Surface and Interface Analysis* 46:393–398.
- [166] Terry AJ, Brown CA (1997) A Comparison of Topographic Characterization Parameters in Grinding. *Annals of the CIRP—Manufacturing Technology* 46(1):479–500.
- [167] Theisel H, Rossi C, Zayer R, Seidel H-P (2004) Normal Based Estimation of the Curvature Tensor for Triangular Meshes, Computer Graphics and Applications, PG 2004. *Proceedings of the 12th Pacific Conference on Computer Graphics and Applications*, 6–8 October 2004, 288–297.
- [168] Thomas TR, Rosén BG (2000) Determination of the Optimum Sampling Interval for Rough Contact Mechanics. *Tribology International* 33(9):601–610.
- [169] Thomas TR, Rosén B-G, Amini N (1999) Fractal Characterisation of the Anisotropy of Rough Surfaces. *Wear* 232(1):41–50.
- [170] Thompson A, Senin N, Giusca C, Leach R (2017) Topography of Selectively Laser Melted Surfaces: A Comparison of Different Measurement Methods. *CIRP Annals* 66(1):543–546.
- [171] Thompson MK, Moroni G, Vanekter T, Fadel G, Campbell RI, Gibson I, Bernard A, Schulz J, Graf P, Ahuja B, Martina F (2016) Design for Additive Manufacturing: Trends, Opportunities, Considerations, and Constraints. *Annals of the CIRP—Manufacturing Technology* 65(2):737–760.
- [172] Todhunter LD, Leach R, Lawes SDA (2017) Results of an Industrial Survey on the Use of Surface Texture Parameters. *16th International Conference on Metrology and Properties of Engineering Surfaces*, poster.
- [173] Townsend A, Pagani L, Blunt L, Scott PJ, Jiang X (2017) Factors Affecting the Accuracy of Areal Surface Texture Data Extraction from X-ray CT. *CIRP Annals* 66(1):547–550.
- [174] Townsend A, Pagani L, Scott P, Blunt L (2017) Areal Surface Texture Data Extraction from X-ray Computed Tomography Reconstructions of Metal Additively Manufactured Parts. *Precision Engineering* 48:254–264.
- [175] Ulcickas V (2000) Using Area-scale Relations to Investigate Measured Fracture Toughness in Y-TZP Materials. *Ceramic Transactions (USA)* 122:211–224.
- [176] Underwood EE, Banerji K (1986) Fractals in Fractography. *Materials Science and Engineering* 80(1):1–14.
- [177] Ungar PS (2015) Mammalian Dental Function and Wear: A Review. *Biosurface and Biotribology* 1:25–41.
- [178] Ungar PS (2017) Tooth Surface Topography: A Scale-sensitive Approach with Implications for Inferring Dental Adaptation and Diet, in Anemone R, Conroy G, (Eds.) *New Geospatial Approaches in Anthropology*, SAR, Press, Santa Fe, NM.
- [179] Ungar PS, Merceron G, Scott RS (2007) Dental Microwear Texture Analysis of Varswater Bovids and Early Pliocene Paleoenvironments of Langebaanweg, Western Cape Province, South Africa. *Journal of Mammalian Evolution* 14(3):163–181.
- [180] Ungar PS, Scott JR, Schubert BW, Stynder DD (2010) Carnivoran Dental Microwear Textures: Comparability of Carnassial Facets and Functional Differentiation of Postcanine Teeth. *Mammalia* 74(2):219–224.
- [181] Usery EL, Finn MP, Scheidt DJ, Ruhl S, Beard T, Bearden M (2004) Geospatial Data Resampling and Resolution Effects on Watershed Modeling: A Case Study Using the Agricultural Nonpoint Source Pollution Model. *Journal of Geographical Systems* 6:289–306.
- [182] Van Valkenburgh B, Teaford MF, Walker A (1990) Molar Microwear and Diet in Large Carnivores: Inferences Concerning Diet in the Sabretooth Cat, *Smilodon fatalis*. *Journal of Zoology* 222:319–340.
- [183] Vessot K, Messier P, Hyde JM, Brown CA (2015) Correlation Between Gloss Reflectance and Surface Texture in Photographic Paper. *Scanning* 37(3):204–217.
- [184] Vulliez M, Gleason MA, Souto-Lebel A, Quinsat Y, Lartigue C, Kordell SP, Lemoine AC, Brown CA (2014) Multiscale Curvature Analysis and Correlations with the Fatigue Limit on Steel Surfaces after Milling. *Procedia CIRP* 13:308–313.
- [185] Walker A, Teaford M (1989) Inferences from Quantitative Analysis of Dental Microwear. *Folia Primatologica International Journal of Primatology* 53(1–4):177–189.
- [186] Wang J, Leach RK, Jiang X (2015) Review of the Mathematical Foundations of Data Fusion Techniques in Surface Metrology. *Surface Topography: Metrology and Properties* 3(2):023001.
- [187] Watson AS, Gleason MA (2016) A Comparative Assessment of Texture Analysis Techniques Applied to Bone Tool Use-wear. *Surface Topography: Metrology and Properties* 4(2):1–18.
- [188] Whitehouse DJ (1982) The Parameter Rash—Is There a Cure? *Wear* 83(1):75–78.
- [189] Whitehouse DJ (2010) *Handbook of Surface and Nanometrology*, CRC Press, Boca Raton, FL.
- [190] Whitehouse DJ, Bowen DK, Venkatesh VC, Lonardo P, Brown CA (1994) Gloss and Surface Topography. *Annals of the CIRP—Manufacturing Technology* 43(2):541–549.
- [191] Workman MJ, Serov A, Halevi B, Atanassov P, Artyushkova K (2015) Application of the Discrete Wavelet Transform to SEM and AFM Micrographs for Quantitative Analysis of Complex Surfaces. *Langmuir* 31(17):4924–4933.
- [192] Yagüe-Fabra JA, Ontiveros S, Jiménez R, Chitchian S, Tosello G, Carmignato S (2013) A 3D Edge Detection Technique for Surface Extraction in Computed Tomography for Dimensional Metrology Applications. *Annals of the CIRP—Manufacturing Technology* 62(1):531–534.
- [193] Young GC, Dey S, Rogers AD, Exton D (2017) Cost and Time-effective Method for Multiscale Measures of Rugosity, FD, and Vector Dispersion from Coral Reef 3D Models. *PLoS One* 12(4):e0175341.
- [194] Zahouani H, El Mansori M (2013) *Multiscale Signature of Surface Topography: Characterization of Areal Surface Texture*, Springer: 217–267.
- [195] Zahouani H, El Mansori M (2017) Multiscale and Multi-fractal of Abrasive Wear Signature of Honing Process. *Wear* 376–377, Part A: 178–87.
- [196] Zahouani H, Lee S-H, Vargiu R (1999) *The Multiscale Mathematical Microscopy of Surface Roughness, Incidence in Tribology, Lubrication at the Frontier: The Role of the Interface and Surface Layers in the Thin Film and Boundary Regime*, Elsevier Science B.V.: 379–390.
- [197] Zahouani H, Mezghani S, Vargiu R, Dursapt M (2005) Multi-scale Study of Abrasion Signature By 2D Wavelet Decomposition. *World Tribology Congress III*, American Society of Mechanical Engineers: 839–840.
- [198] Zahouani H, Mezghani S, Vargiu R, Dursapt M (2008) Identification of Manufacturing Signature by 2D Wavelet Decomposition. *Wear* 264(5):480–485.
- [199] Zeng W, Jiang X, Scott P (2005) Metrological Characteristics of Dual Tree Complex Wavelet Transform for Surface Analysis. *Measurement Science and Technology* 12(7):1410–1417.
- [200] Zeng Y, Wang K, Wang B, Brown CA (2014) Multiscale Evaluations of the Roughness of Surfaces Made by Additive Manufacturing. *ASPE-2014 Spring Topical Meeting*.
- [201] Zhang X, Drake NA, Wainwright J, Mulligan M (1999) Comparison of Slope Estimates from Low Resolution DEMs: Scaling Issues and a Fractal Method for Their Solution. *Earth Surface Processes and Landforms* 24(9):763–779.
- [202] Zhang B, Liu X, Brown CA, Bergstrom TS (2002) Microgrinding of Nanostructured Material Coatings. *Annals of the CIRP—Manufacturing Technology* 51(1):251–254.
- [203] Zhang H, Wang Y, Janis CM, Goodall RH, Purnell MA (2017) An Examination of Feeding Ecology in Pleistocene Proboscideans from southern China (Sino-mastodon, Stegodon Elephas), by Means of Dental Microwear Texture Analysis. *Quaternary International* 445:60–70.

- [204] Zhang X, Xu Y, Jackson RL (2017) An Analysis of Generated Fractal and Measured Rough Surfaces in Regards to Their Multiscale Structure and FD. *Tribology International* 105:94–101.
- [205] Zheng SY, Zheng J, Gao SS, Yu BJ, Yu HY, Qian LM, Zhou ZR (2011) Investigation on the Microtribological Behaviour of Human Tooth Enamel by Nanoscratch. *Wear* 271(9–10):2290–2296.
- [206] Bruzzone AAG, Montanaro JS, Ferrando A, Lonardo PM (2004) Wavelet Analysis for Surface Characterisation: an Experimental Assessment. *CIRP Annals—Manufacturing Technology* 53(1):479–482.
- [207] He L, Evans CJ, Davies A (2012) Two-quadrant Area Structure Function Analysis for Optical Surface Characterization. *Optics Express* 20 (21):23275–23280.
- [208] He L, Evans CJ, Davies A (2013) Optical Surface Characterization with the Area Structure Function. *CIRP Annals* 62:539–542.
- [209] Hvisic AM, Burge JH (2007) in Burge JH, Faehnle OW, Williamson R, (Eds.) *Structure Function Analysis of Mirror Fabrication and Support Errors*, . <http://dx.doi.org/10.1117/12.736051>p. 66710A.
- [210] ISO, D, 10110-8: *Optics and Optical Instruments—Preparation of Drawings for Optical Elements and Systems*.
- [211] Parks, RE (2008), September. Specifications: Figure and Finish are not enough. In *An optical Believe It or Not: Key Lessons Learned* (Vol. 7071, p. 70710B). International Society for Optics and Photonics.

## Additional references